General Disclaimer

One or more of the Following Statements may affect this Document

- This document has been reproduced from the best copy furnished by the organizational source. It is being released in the interest of making available as much information as possible.

- This document may contain data, which exceeds the sheet parameters. It was furnished in this condition by the organizational source and is the best copy available.

- This document may contain tone-on-tone or color graphs, charts and/or pictures, which have been reproduced in black and white.

- This document is paginated as submitted by the original source.

- Portions of this document are not fully legible due to the historical nature of some of the material. However, it is the best reproduction available from the original submission.

NASA TECHNICAL MEMORANDUM

NASA TM X- 72698

NASA TM X- 72698

EFFECTS OF INLET TREATMENT LOCATION AND TREATMENT CAVITY DEPTH ON COMPRESSOR NOISE

BY

Lorenzo R. Clark

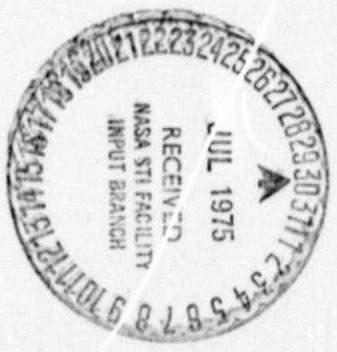

June 1975

NATIONAL AERONAUTICS AND SPACE ADMINISTRATION
LANGLEY RESEARCH CENTER, HAMPTON, VIRGINIA 23665

1. Report No.	2. Government Accession No.	3. Recipient's Catalog No.
TM X-72698		

4. Title and Subtitle	5. Report Date
EFFECTS OF INLET TREATMENT LOCATION AND TREATMENT CAVITY DEPTH ON COMPRESSOR NOISE	June 10, 1975
	6. Performing Organization Code: 26.400
7. Author(s): Lorenzo R. Clark	8. Performing Organization Report No.
9. Performing Organization Name and Address: Langley Research Center, Hampton, Virginia 23665	10. Work Unit No.: 505-03-12-04
	11. Contract or Grant No.
12. Sponsoring Agency Name and Address: National Aeronautics and Space Admiistration, Washington, D. C. 20546	13. Type of Report and Period Covered: Technical Memorandum
	14. Sponsoring Agency Code

15. Supplementary Notes

16. Abstract

An experimental study of the ability of acoustic liners to reduce compressor noise inside and in front of an inlet has been made. An axial flow research compressor and a specially designed inlet were used to make the investigation inside an anechoic chamber. Acoustic and performance data were obtained for a range of inlet treatment locations and cavity depths in order to determine their effects on inlet noise over a range of blade passing frequencies.

The greatest noise reductions in front of the inlet were obtained with acoustic treatment located close to the compressor and backed with the deepest cavities tested. Inside the inlet the maximum noise level reductions were obtained in the area of the treatment regardless of treatment location. No appreciable losses in compressor performance were measured.

17. Key Words (Suggested by Author(s)) (STAR category underlined)	18. Distribution Statement
Acoustics, compressor noise, inlet, acoustic treatment, noise reduction, compressor performance.	Unclassified Unlimited

19. Security Classif. (of this report)	20. Security Classif. (of this page)	21. No. of Pages	22. Price*
U	U	42	$3.75

*Available from { The National Technical Information Service, Springfield, Virginia 22151 / STIF/NASA Scientific and Technical Information Facility, P.O. Box 33, College Park, MD 20740

EFFECTS OF INLET TREATMENT LOCATION AND TREATMENT CAVITY DEPTH ON COMPRESSOR NOISE

by

Lorenzo R. Clark
Langley Research Center

SUMMARY

Studies have been undertaken to evaluate the effects of acoustic lining backing depth and location on the reduction of compressor noise inside and in front of an inlet. A one-stage transonic axial-flow research compressor with a specially designed inlet was used in this investigation. Information regarding effects of the treatment on compressor performance is also included.

These model studies suggest that by increasing backing depth and locating the treatment close to the compressor face large noise reductions of the blade passing frequencies are measured in the far field. On the other hand, location of inlet treatment further upstream from the compressor face appears to alter this overall effect noticeably. At the lowest blade passing frequency noise level reductions inside the treated region of the duct were found to increase directly with increasing backing depth regardless of treatment location. However, noise levels measured at the highest blade passing frequency indicated that there is an optimum backing depth with which noise reductions may be obtained inside the treated area. Generally, no measurable lossess were found in compressor performance.

INTRODUCTION

Much research has been done regarding the reduction of fan noise from turbofan engines (see refs. 1 to 10). In each of these studies noise level reduction of discrete tones has been obtained through the application of acoustic liners. It has been shown that the effectiveness of the acoustic material depends on treatment cavity depth, duct height or separation between treated surfaces, and frequency of peak attenuation (see refs. 11 to 13). Most of the work has involved materials that perform satisfactorily at frequencies associated with the blade passing frequency of rotation. Some of these studies have also provided useful information on the performance penalties associated with inlet treatment applications (see refs. 6 to 9).

This paper presents acoustic and performance data from tests of a model compressor in which cavity depth and treatment location were varied in order to determine their effect on a range of blade passing frequency related noise levels inside and in front of an inlet duct. The primary purpose of the paper is to provide a documentation of inlet noise data obtained experimentally for comparison with the findings of similar research efforts. In the future, substantial improvements in the prediction of liner effectiveness should occur as the influence of parameters investigated in this study are better understood.

SYMBOLS

ρc	specific acoustic impedance of air, newton-second/meter^3 (pound force-second/feet^3)
$\bar{R}$	real part (resistance)of normalized specific acoustic impedance, newton-second/meter^3 (pound force-second/feet^3)
$\bar{X}$	imaginary part (reactance) of normalized specific acoustic impedance, newton-second/meter^3 (pound force-second/feet^3)
$\bar{Z}$	specific acoustic impedance normalized to ρc, $(R + iX)/\rho c$

Abbreviations:

dB	decibels, re 0.0002 microbars
FBPF	first blade passing frequency, rpm x 29/60, Hertz
SPL	sound pressure level, decibels

APPARATUS AND PROCEDURE

Description of Research Inlet

The compressor inlet used in these studies was fabricated especially for duct treatment noise research studies and is shown in figures 1 and 2. The inlet is made of aluminum and consists of two separable parts, a bellmouth section and an acoustically treatable section. All calculations were made with English units in this report. The treatable section is 0.57 m (22.4 in.) long, has a 0.41 m (16 in.) inside diameter, and is constructed such that it will accommodate up to 0.46 m (18 in.) of acoustical treatment in circular sections.

Six treated inlet configurations were tested in the present study. Three of these were formed by first inserting a 0.23 m (9 in.) treated section and then a 0.23 m (9 in.) untreated section in the inlet. The remaining configurations were formed by reversing this procedure. Each downstream insert occupied a position 0.51 m (20 in.) upstream of the compressor rotor. Each upstream insert was located 0.74 m (29 in.) upstream of the compressor rotor. The treated ring inserts used in these studies are shown in figure 3. Each liner was of the following construction: type 347 stainless steel fibermetal inner wall, fiberglass outer wall, and fiberglass honeycomb core with a specified cavity depth sandwiched between the walls. Three honeycomb cell depths, 3.2 mm (1/8 in.), 6.4 mm (2/8 in.), and 9.5 mm (3/8 in.), were chosen for these tests from calculations which indicated that the 9.5 mm (3/8 in.) deep cavities were best tuned for attenuating discrete noise over frequencies ranging from 8000 Hz to 10 000 Hz. A photograph of

samples showing the fibermetal and honeycomb cell structures is presented in figure 4. Acoustical properties of the fibermetal are discussed in the appendix.

Description of Research Compressor

The noise source used in the present studies was an experimental compressor manufactured especially for noise research studies and is shown in figure 1. It is an axial-flow machine having a design airflow of 11.32 kg/sec (25 lb/sec) at a pressure ratio of 3. It has three rotor stages designed for transonic operation with a design corrected rotational speed of 24 850 rpm. The maximum power absorbed by the compressor is 2350 hp (1752 KW). The compressor has a design rated efficiency of 82 percent. It is designed to operate as a one-, two-, or three-stage machine, and provision is made for changing the number of rotor blades and stator vanes. The one-stage transonic configuration was used in this investigation. Additional design information is given in reference 14.

Noise Instrumentation and Measurement

The microphone locations are shown in figure 2. One 12.7 mm (0.5 in.) diameter condenser microphone (microphone 1) was attached to a traversing boom. The boom traversed 0^{o} to 90^{o} about the compressor centerline in the horizontal plane to obtain sound radiation patterns. Data were obtained with this microphone at a distance of 3.05 m (10 ft) from the inlet bell. The microphone was set at the same elevation as the compressor centerline with its diaphragm in the vertical plane. Five 12.7 mm (0.5 in.) diameter

microphone holes were drilled through the walls of the inlet treatable section along a line perpendicular to the inlet face, for the purpose of measuring noise levels inside the duct. One of these microphone holes was located in the rear of the treatable section. The remaining holes were also drilled through the ring inserts such that two holes entered each ring 5.1 cm (2 in.) from its ends. The locations of these microphone holes are indicated in figure 3. Two 12.7 mm (0.5 in.) diameter condenser microphones, microphone 2 at 0.81 m (31.5 in.) upstream of the compressor rotor and microphone 3 at 0.57 m (22.5 in.) upstream of the compressor rotor, were mounted along the inlet treatable section. An identical type microphone (microphone 4) was mounted on the inlet treatable section between the downstream insert and the compressor - i.e., 0.46 m (18.25 in.) upstream of the rotor - for measuring reference levels. All unused microphone holes were plugged during data collection. It was assumed in this study that the bellmouth section was sufficient to render the compressor inlet relatively non-reflecting.

The overall frequency response of the recording system was flat within $\pm$2 dB from 500 Hz to 40 000 Hz. The entire sound-measurement system was calibrated before and after data collection by means of a discrete frequency calibrator. Each microphone provided data for 1/10-octave spectral analyses.

Compressor Operating Procedures

After routine operating procedures were performed, the compressor speed was increased to 15 500 rpm (FBPF = 7500 Hz). At this speed, the back-pressure valves (primary and vernier) were set to yield a pressure ratio reading of 1.12. This was considered to be a realistic operating condition with reasonable compressor efficiencies. After all temperatures and pressures stabilized, the compressor was considered to be operating at thermodynamic equilibrium. The compressor was then increased to 16 560 rpm (FBPF = 8000 Hz), without further adjustment to the back-pressure valves. Performance and noise data were taken during a 5-minute stabilized run. This procedure was repeated in increments of 500 Hz for other compressor speeds up to 20 700 rpm (FBPF = 10 000 Hz). The calculated maximum axial Mach number in the inlet guide vanes is 0.58 at this upper operating speed. Therefore, according to reference 14, inlet choking effects were not a factor in these tests.

It should be noted that much effort was made to have the compressor radiate identical noise levels at the reference microphone for comparable operating conditions using untreated and treated inlets. However, reference levels were found to differ appreciably in a few cases.

Performance Instrumentation and Measurement

The instrumentation used to measure performance data was generally the same as that described in reference 14. Six thermocouple probes were equally spaced, circumferentially, in the inlet bellmouth. The outputs from these probes were averaged to obtain the inlet air temperature which was

used to determine inlet enthalpy and speed of sound in air. Three static pressure ports were located at the entrance to the rotor housing. The average output of these ports and the barometric pressure provided enough information to obtain airflow in Kg/sec (lb/sec) from a calibration curve provided by the compressor manufacturer. Discharge pressures were obtained from the average of three pressure probes built into struts located in the discharge section of the compressor. Compressor pressure ratio was calculated from discharge pressure divided by barometric pressure. All pressure measurements were read from pressure gauges. Discharge temperatures were obtained from thermocouple probes also built into the struts in the discharge section of the compressor. Enthalpies of the air leaving the compressor were determined from averages of the discharge temperatures. Compressor efficiencies were then determined by using the inlet and outlet enthalpies found from inlet and outlet temperatures and isentropic enthalpies determined by use of the pressure ratio values. Compressor rotational speed was determined by use of a magnetic pickup and was displayed on an electronic counter in rpm.

RESULTS AND DISCUSSION

The main variables of the tests were acoustic lining backing depth and duct lining location. For each test condition, overall sound pressure levels, radiation patterns, fundamental-blade-passing-frequency sound pressure levels, and compressor performance measurements were obtained.

Noise Measurements

Noise measurements inside compressor inlet.- Data obtained at the extreme test frequencies were found to represent the SPL trends measured inside the duct. Sample 1/10-octave band relative noise levels measured at each of the

three inlet microphone locations are plotted in figures 5 and 6 for the various honeycomb backing depths investigated at 8000 Hz. Figure 5 shows a comparison of relative FBPF SPL for configurations without treatment and with treatment located at the downstream end of the inlet treatable section. Examination of the curve obtained with the untreated inlet shows no noise reduction below the reference level at microphones 3 and 2. Adding treatment, however, showed attenuated noise levels at microphones 3 and 2 for each honeycomb backing depth used. The greatest noise level reduction, 9 dB, is seen to occur at the number 3 microphone in the inlet lined with 9.5 mm (3/8 in.) deep honeycomb cells. Figure 6 shows a comparison of relative FBPF SPL for configurations without treatment and with treatment located at the upstream end of the inlet treatable section. Again the data obtained with the untreated inlet show no attenuation at microphones 3 and 2 compared with the reference level. The insertion of each acoustic liner resulted in noise level reductions at microphone 3, but the greatest attenuation, 12 dB, was measured at microphone 2 in the presence of acoustic treatment backed with 9.5 mm (3/8 in.) deep honeycomb cells.

Presented in figures 7 and 8 are 10 000 Hz data measured inside the inlet using each inlet configuration. Figure 7 shows a comparison of relative FBPF SPL for configurations without treatment and with treatment located at the downstream end of the inlet treatable section. Like figures 5 and 6, figure 7 shows the compressor noise attenuated at microphones 3 and 2 with each backing depth. Here the greatest attenuations, 9 dB at microphone 3 and 8 dB at microphone 2, are accomplished with the treatment having a 6.4 mm (2/8 in.) honeycomb backing depth. Figure 8 shows how placing the three

acoustic ring inserts upstream affects noise propagating through the inlets. It can be seen that no noise level reduction is achieved at microphone 3 in the absence of treatment. On the other hand, microphone 2 shows a sizable decrease in noise level at the treated end of each inlet configuration. A maximum attenuation of 16 dB was obtained with the 6.4 mm (2/8 in.) deep honeycomb cells.

It should be mentioned that in most cases where data obtained with untreated and treated inlets were compared the reference microphone levels inside the respective ducts were approximately the same. This is indicated by the peak sound pressure levels plotted on a vertical scale in figures 5 to 20. As figure 8 indicated, however, some comparisons between untreated and treated inlet data did show noticeable differences in reference microphone levels. Nevertheless, it should be remembered that in all cases where data obtained with untreated and treated inlets were compared the compressor speed and back pressure were essentially identical. Therefore, the total noise propagating through the inlets in these cases should have been essentially the same. Contrary to the non-reflecting behavior of the inlet assumed earlier, the differences in reference levels measured inside the untreated and treated inlet configurations are thought to be primarily the results of noise reflections inside the downstream entrance to the inlet.

Although they are not presented, curves similar to those shown in figures 5 through 8 were plotted for the 8500, 9000, and 9500 Hz cases. The combined results showed attenuations inside each treated inlet in the region of treatment, but the liner with 6.4 mm (2/8 in.) deep honeycomb cells demonstrated a slightly greater noise reducing ability.

Radiation patterns.- Radiation patterns were obtained at each compressor operating condition. The data for each pattern were obtained with the use of a traversing microphone in the front quadrant from 0^{o} (on the axis) to 90^{o}. Beginning with the low end of the frequency range at which the compressor was operated, figure 9 compares the relative FBPF SPL obtained with the untreated inlet to those obtained with each inlet configuration having downstream treatment at 8000 Hz. It can be seen that noise level reductions were obtained at various azimuthal angles with each treated inlet, but there were also azimuthal angles at which the treated inlets radiated higher noise levels than those radiated by the untreated inlet. The biggest attenuation, 8 dB, was obtained at the 75^{o} azimuthal angle with each treated inlet.

Relative FBPF SPL obtained with the untreated inlet and those obtained with the three inlet configurations having upstream treatment at 8000 Hz are compared in figure 10. Except for a 1 db increase in noise level at 0^{o} with the inlet having 3.2 mm (1/8 in.) deep honeycomb backing and a 2 dB increase in noise level at 30^{o} with the inlet having a 9.5 mm (3/8 in.) deep backing, each treated inlet showed a reduction in noise level at each azimuthal angle. If the relatively high absolute level (88 dB) measured at 90^{o} with the latter configuration is also excepted it is seen that substantial noise level reductions are obtained with each treated inlet at the larger azimuths. Maximum attenuations of 12 dB, 19 dB, and 17 dB were obtained at 75^{o} with the 3.2 mm (1/8 in.), 6.4 mm (2/8 in.), and 9.5 mm (3/8 in.) backing depths, respectively.

Figures 11 through 13 show comparisons of relative FBPF SPL radiated by the untreated inlet and the inlets with downstream treatment at the intermediate test frequencies 8500 Hz, 9000 Hz, and 9500 Hz, respectively. Again noise level reductions were accomplished at various azimuths with each acoustically lined duct. However, the noise level was most significantly attenuated at 8500 and 9000 Hz with the inlet containing 9.5 mm (3/8 in.) deep cells.

Noise patterns which radiated from the untreated inlet are compared to radiations from the inlets with upstream treatment at 8500, 9000, and 9500 Hz in figures 14, 15, and 16, respectively. Figure 14 shows that maximum noise level decreases of 7 db at 75^{o} and 6 dB at 15^{o} were obtained with the 6.4 mm (2/8 in.) and 9.5 mm (3/8 in.) backing depths, respectively. Virtually no attenuation was achieved with the remaining acoustic duct. In fact, the noise radiated from it exceeded the reference level by as much a 7 dB at the 75^{o} azimuthal angle. Substantially greater noise level reductions were accomplished at 9000 Hz and 9500 Hz with each inlet configuration (see figs. 15 and 16). Except for modest increases in noise level at the 15^{o} azimuthal angle with the 6.4 mm (2/8 in.) and 9.5 mm (3/8 in.) backing depths, attenuations were achieved throughout the azimuthal range at these frequencies. At 9000 Hz the inlets with 6.4 mm (2/8 in.) and 9.5 mm (3/8 in.) deep treatment backing reduced the noise level at 75^{o} by 10 dB. At 9500 Hz the biggest attenuation, 13 dB at the 60^{o} azimuth, was obtained with the 3.2 mm (1/8 in.) backing depth.

Figures 17 and 18 show comparisons of relative FBPF SPL for the

untreated and treated inlet configurations at the highest test frequency (10 000 Hz). Radiation patterns are presented in figure 17 for the untreated inlet and the inlet with downstream treatment. At this frequency it is seen that the compressor noise is reduced at each azimuthal angle with each inlet configuration. Peak attenuations of 12 dB were measured at the 0^{o} and 45^{o} azimuthal angles for the 9.5 mm (3/8 in.) deep honeycomb cell configuration. Peak attenuations of 10 dB and 9 dB were measured at the 45^{o} and 0^{o} azimuths for the 3.2 mm (1/8 in.) and 6.4 mm (2/8 in.) deep honeycomb cell configurations, respectively. Figure 18 compares radiation patterns for the untreated inlet and the inlet with upstream treatment. Again, the figure shows that the compressor noise was attenuated with each treated configuration throughout the range of azimuthal angles traversed. However, the inlet with 6.4 mm (2/8 in.) treatment backing proved to be a better noise attenuator than its two competitors. A maximum attenuation of 12 dB was obtained with this inlet at 15^{o}. The inlet with 3.2 mm (1/8 in.) treatment backing gave the next best performance with regard to achievement of noise reduction. It reduced the compressor noise 9 dB at 45^{o}.

A comparison at FBPF = 10 000 Hz of 1/10-octave noise spectra obtained with the boom microphone at 0^{o} is made in figure 19 for the compressor inlet untreated and with downstream treatment backed with 9.5 mm (3/8 in.) deep cavities. These spectra show the noise radiated from the treated inlet significantly reduced at each frequency.

Figure 20 shows a comparison at FBPF = 10 000 Hz of 1/10 octave noise spectra obtained with the boom microphone at 15^{o} for the inlet untreated and

6.4 mm (2/8 in.) deep cavities. Here, the noise radiated from the treated inlet is reduced significantly at only the middle and upper frequencies of the spectra.

Compressor Performance

Effects of downstream and upstream inlet treatment on the compressor performance are indicated in tables I and II, respectively. Listed in the tables are values of compressor pressure ratio and efficiency as computed for each inlet configuration and blade passing frequency. The pressure ratios given in each table were obtained without adjustment to the back-pressure valve. Both tables show virtually no loss in compressor pressure ratio due to acoustical modification of the compressor inlet. Some variations can be seen in compressor efficiency due to the addition of both downstream and upstream inlet treatment; however, only the inlet equipped with 9.5 mm (3/8 in.) deep honeycomb cells in the downstream position effected compressor efficiency losses at each BPF, an average loss of 2.6 percent over the entire frequency range.

CONCLUDING REMARKS

An investigation has been conducted to determine the effects of acoustic treatment location and backing depth on noise radiated inside and in front of a one-stage-transonic-axial-flow-research compressor inlet. Compressor performance and noise measurements were made over a range of frequencies during tests of three treatment backing depths at two inlet locations.

Noise levels measured inside the various inlet configurations yielded the following results:

1. The greatest noise level reductions were achieved inside the treated region of the inlet at 8000 Hz and 10 000 Hz regardless of treatment location.

2. The treated configurations with 9.5 mm (3/8 in.) and 6.4 mm (2/8 in.) cavity depths gave maximum noise level attenuations at 8000 Hz and 10 000 Hz, respectively.

Noise levels measured in front of the inlet yielded the following results:

1. Noise level reductions were obtained at 10 000 Hz with each inlet configuration at each azimuthal angle traversed regardless of treatment location.

2. Using downstream inlet treatment at 10 000 Hz the maximum noise level attenuations were accomplished at each azimuth with a 9.5 mm (3/8 in.) deep cavity depth. The greatest of these reductions, 12 dB, was accomplished at the 0^{o} and 45^{o} positions.

3. Using upstream inlet treatment at 10 000 Hz the maximum noise level attenuations were accomplished at each azimuthal angle (except for 0^{o} and 30^{o}) with a 6.4 mm (2/8 in.) cavity depth. The greatest of these reductions, 12 dB, was accomplished at the 15^{o} position.

There were no appreciable compressor-efficiency losses due to location of acoustic treatment at either downstream or upstream inlet position. Neither were significant losses in pressure ratio associated with the various inlet configurations.

APPENDIX

Impedance and Flow Resistance of Type 347 Stainless Steel Fibermetal

Normalized specific acoustic impedance. - The specific acoustic impedance of type 347 fibermetal was calculated for various frequencies using data obtained experimentally. Plotted in figure 21 are the resistance (real part) and reactance (imaginary part) of the normalized specific acoustic impedance of a 33.0 mm (1.3 in.) diameter fibermetal sample mounted in the end of an impedance tube. The straight lines drawn through the data were positioned by the calculation technique known as the method of least squares. The extrapolated (dashed) portions of the curves are primarily intended to approximate impedance values of the fibermetal over the frequency range covered in these noise tests, 8000 to 10 000 Hz. Impedance measurements at these frequencies were not obtainable with the laboratory apparatus available.

Flow resistance. - The flow resistance of type 347 fibermetal was calculated for various particle velocities using data obtained experimentally. These results are presented in figure 22. The curve drawn is a visual fit of the data plotted. As can be seen, it shows a continual increase of flow resistance with particle velocity over the range of 0.363 to 3.63 m/sec (1.19 to 11.9 ft/sec).

REFERENCES

1. Progress of NASA Research Relating to Noise Alleviation of Large Subsonic Jet Aircraft. A Conference held at the NASA-Langley Research Center, Hampton, VA, Oct. 8-19, 1968. NASA SP-189.

2. NASA Acoustically Treated Nacelle Program. Conference held at NASA-Langley Research Center, Hampton, VA Oct. 15, 1969. NASA SP-220.

3. Kramer, James J.; Chestnutt, David; Krejsa, Eugene A.; Lucas, James G.; and Rice, Edward J.: Noise Reduction. Presented at Conference on Aircraft Propulsion, NASA Lewis Research Center, Cleveland, OH, Nov. 18-19, 1970, pp. 169-209.

4. Aircraft Engine Noise Reduction. NASA LeRC, Cleveland, OH, May 1972, NASA SP-311.

5. Study and Development of Turbofan Nacelle Modifications to Minimize Fan-Compressor Noise Radiation. Vol. I - Program Summary. NASA CR-1711. The Boeing Company, 1971.

6. Rice, Edward J.; Feiler, Charles E.; and Acker, Loren W.: Acoustic and Aerodynamic Performance of a 6-Foot-Diameter Fan for Turbofan Engines. NASA TN D-6178, 1971.

7. Hodge, C. G.; and Wood, S.K.: The Effect of Inlet-Noise Suppression on Propulsion System Design. Paper 73-1294, AIAA/SAE 9th Propulsion Conf., Las Vegas, Nevada. Nov. 5-7, 1973.

8. Feiler, Charles E.; and Meriman, James E.: Effects of Forward Velocity and Acoustic Treatment on Inlet Fan Noise. NASA TM X-71591, 1974.

9. Dittmar, James H.; and Groeneweg, John F.: Effect of Treated Length on Performance of Full-Scale Turbofan Inlet Noise Suppressors. NASA TN D-7826, 1974.

10. Cornell, W. G.: Experimental Quiet Engine Program - Summary Report. NASA CR-2519, 1975.

11. Marsh, Alan H.; Elias, I.; Hoehne, J.C.; and Frasca, R.L.: A Study of Turbofan-Engine Compressor-Noise Suppression Techniques. NASA CR-1056, 1968.

12. Zorumski, William E.; and Parrott, Tony L.: Nonlinear Acoustic Theory for Rigid Porous Materials. NASA TN D-6196, 1971.

13. Budoff, Marvin; and Zorumski, William E.: Flow Resistance of Perforated

Plates in Tangential Flow. NASA TM X-2361, 1971.

14. Chestnutt, David: Noise Reduction by Means of Inlet-Guide-Vane Choking in an Axial-Flow Compressor. NASA TN D-4682, 1968.

TABLE I.- EFFECTS OF DOWNSTREAM INLET TREATMENT ON COMPRESSOR PERFORMANCE

Inlet configuration	Cell depth		Fundamental frequency, Hz	Compressor pressure ratio	Compressor efficiency, percent
	mm	in.			
Untreated	—	—	8000	1.14	74.7
			8500	1.16	76.1
			9000	1.18	73.6
			9500	1.20	77.2
			10000	1.23	77.3
Treated	3.2	$\frac{1}{8}$	8000	1.14	74.2
			8500	1.16	76.1
			9000	1.18	76.3
			9500	1.20	76.8
			10000	1.23	77.7
Treated	6.4	$\frac{2}{8}$	8000	1.14	76.6
			8500	1.16	74.3
			9000	1.18	77.6
			9500	1.20	76.4
			10000	1.22	79.7
Treated	9.5	$\frac{3}{8}$	8000	1.14	73.8
			8500	1.16	69.9
			9000	1.18	71.8
			9500	1.20	74.4
			10000	1.23	74.1

TABLE II. - EFFECTS OF UPSTREAM INLET TREATMENT ON COMPRESSOR PERFORMANCE

Inlet configuration	Cell depth, mm	Cell depth, in.	Fundamental frequency, Hz	Compressor pressure ratio	Compressor efficiency, percent
Untreated	—	—	8000	1.14	74.7
			8500	1.16	76.1
			9000	1.18	73.6
			9500	1.20	77.2
			10000	1.23	77.3
Treated	3.2	1/8	8000	1.15	72.5
			8500	1.17	76.6
			9000	1.19	77.6
			9500	1.21	79.2
			10000	1.25	82.3
Treated	6.4	2/8	8000	1.14	72.6
			8500	1.17	72.8
			9000	1.19	75.3
			9500	1.21	79.6
			10000	1.25	82.8
Treated	9.5	3/8	8000	1.15	77.4
			8500	1.17	77.7
			9000	1.20	79.9
			9500	1.22	83.4
			10000	1.26	90.0

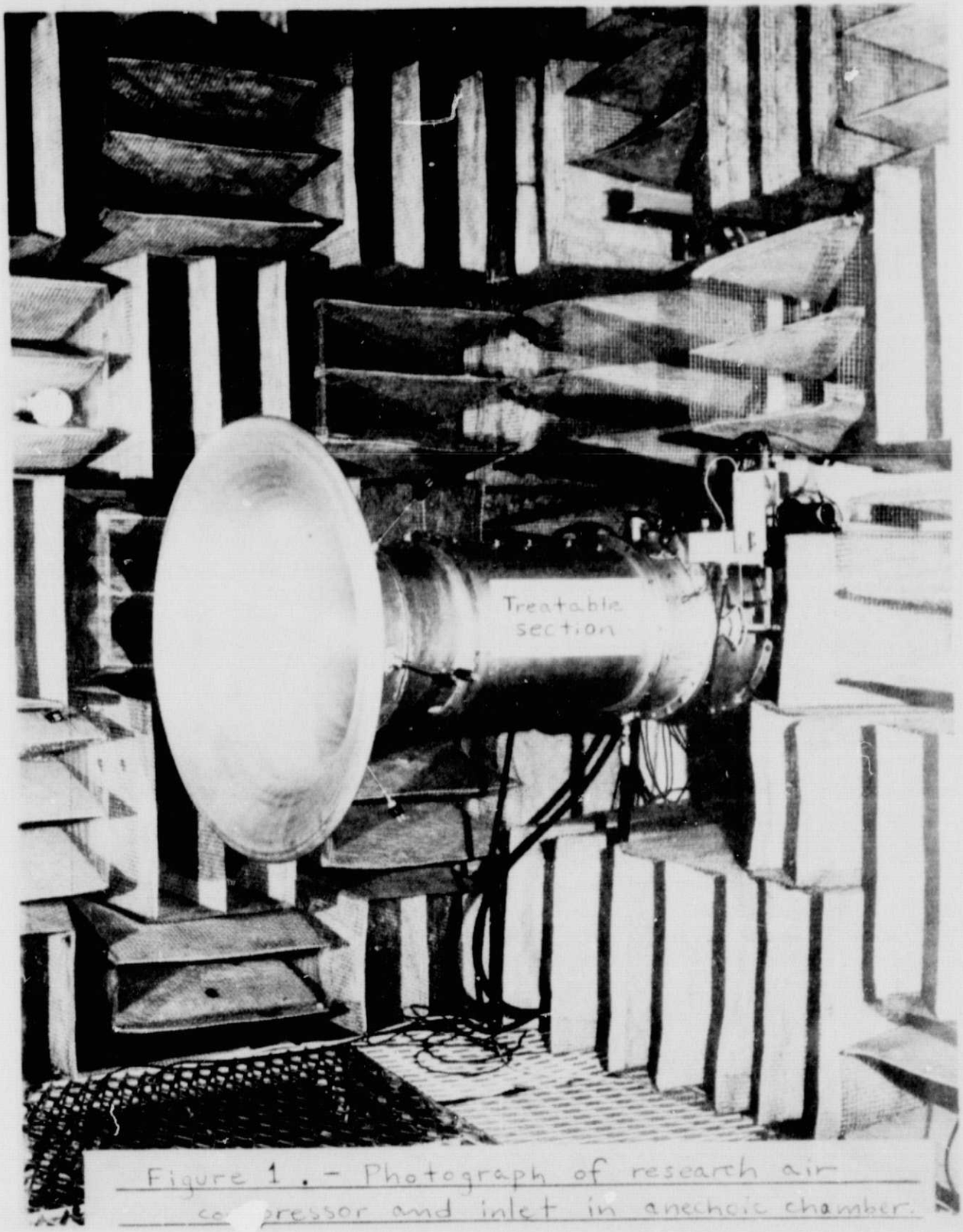

Figure 1. - Photograph of research air compressor and inlet in anechoic chamber.

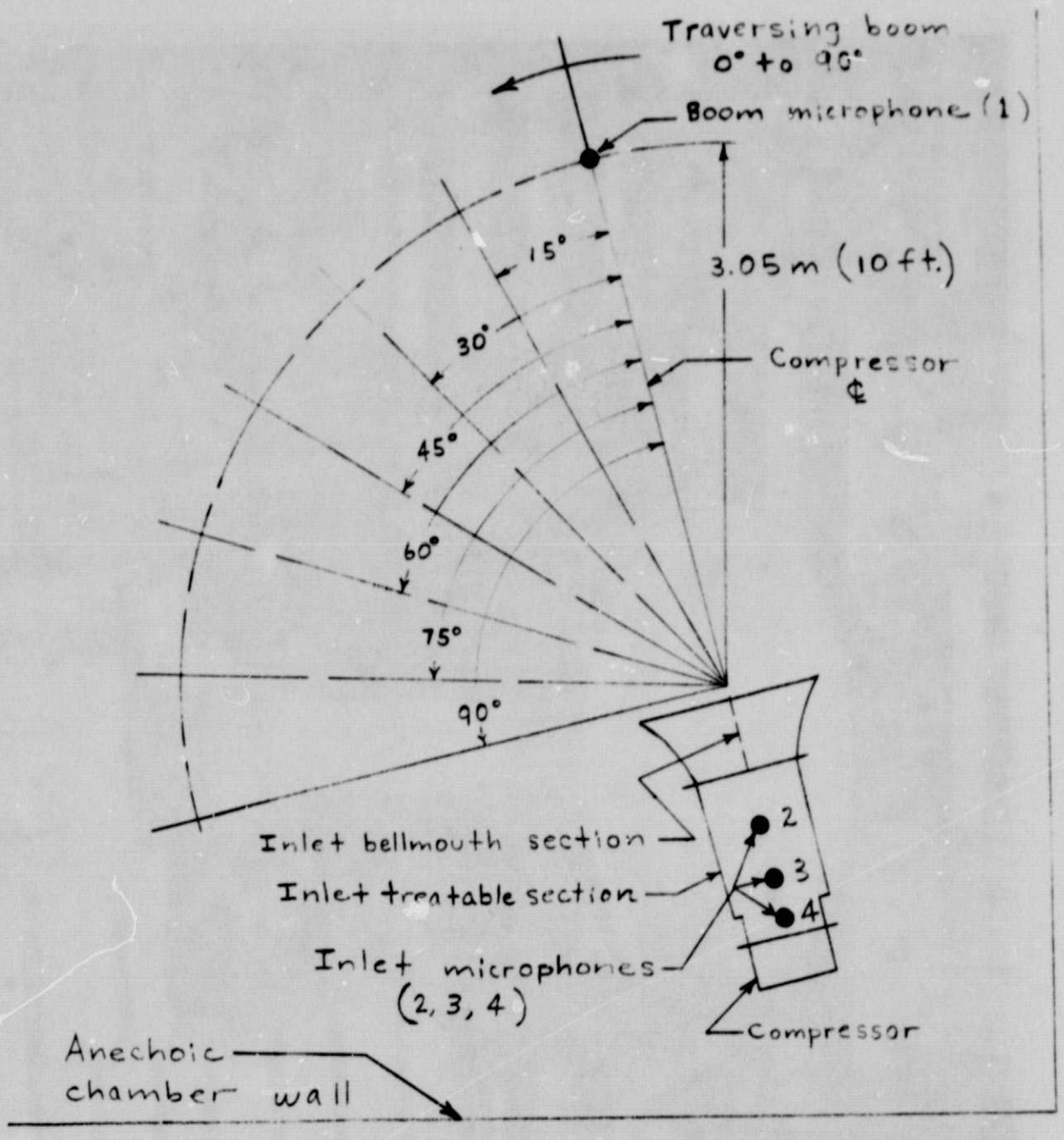

Figure 2 .- Microphone layout.

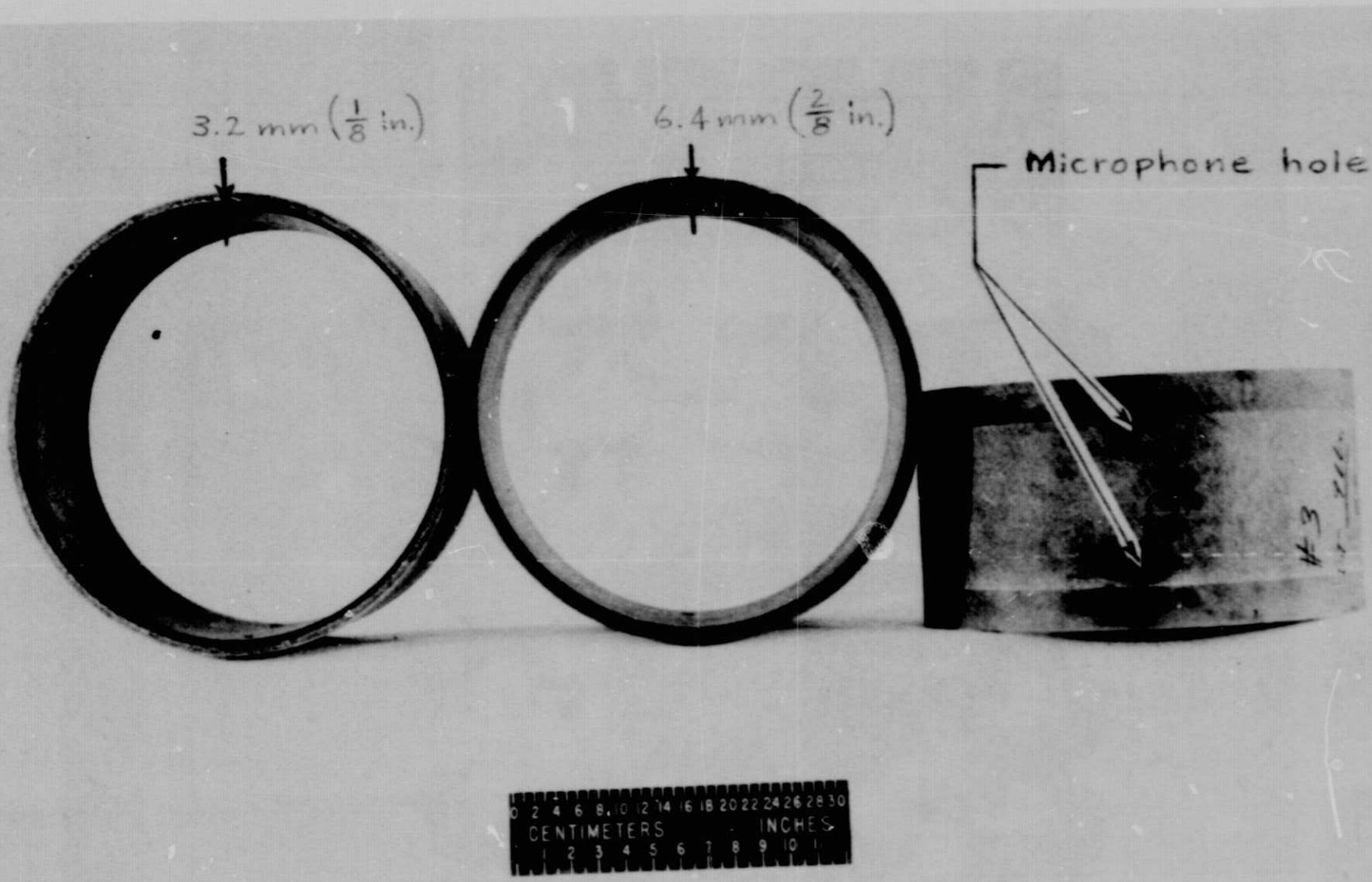

Figure 3 .- Three treated ring inserts and location of microphone holes.

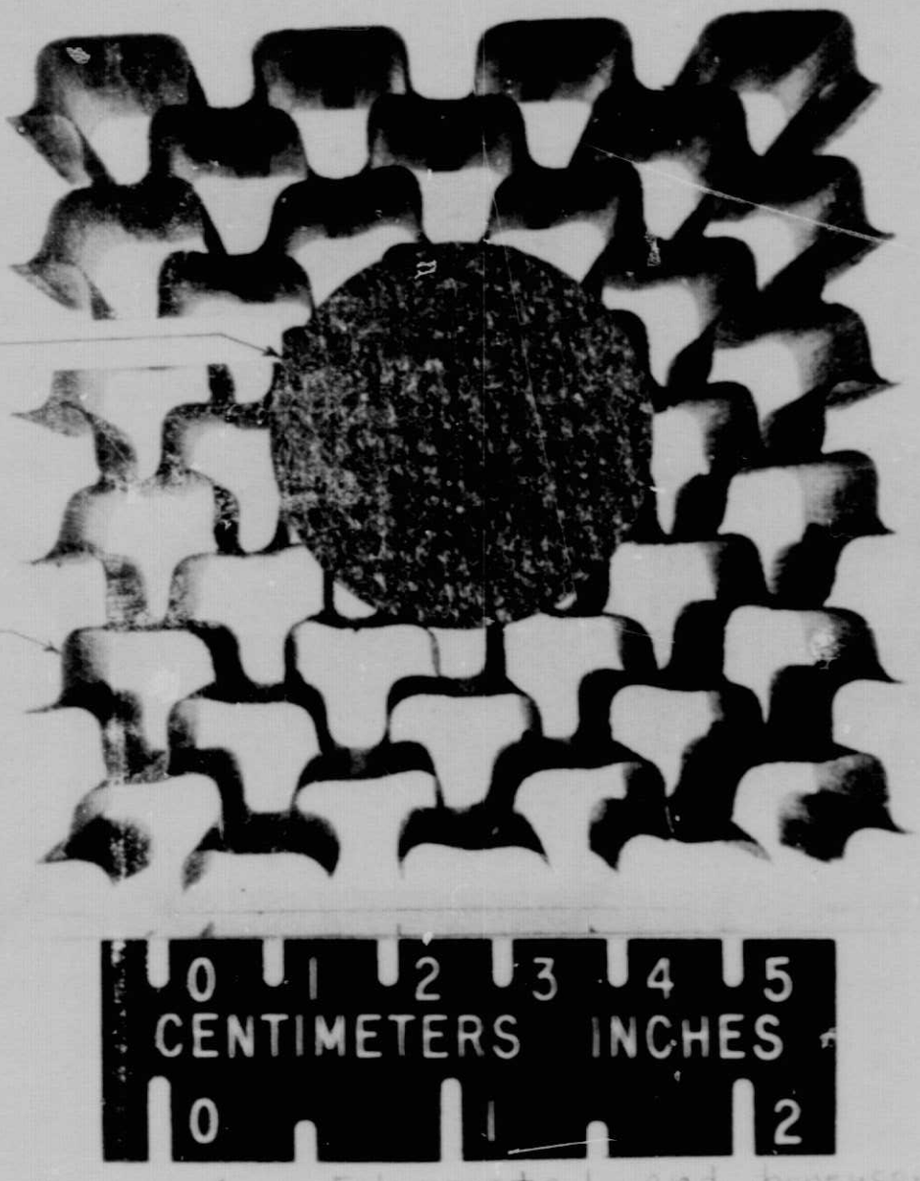

Figure 4. - Fibermetal and honeycomb backing samples.

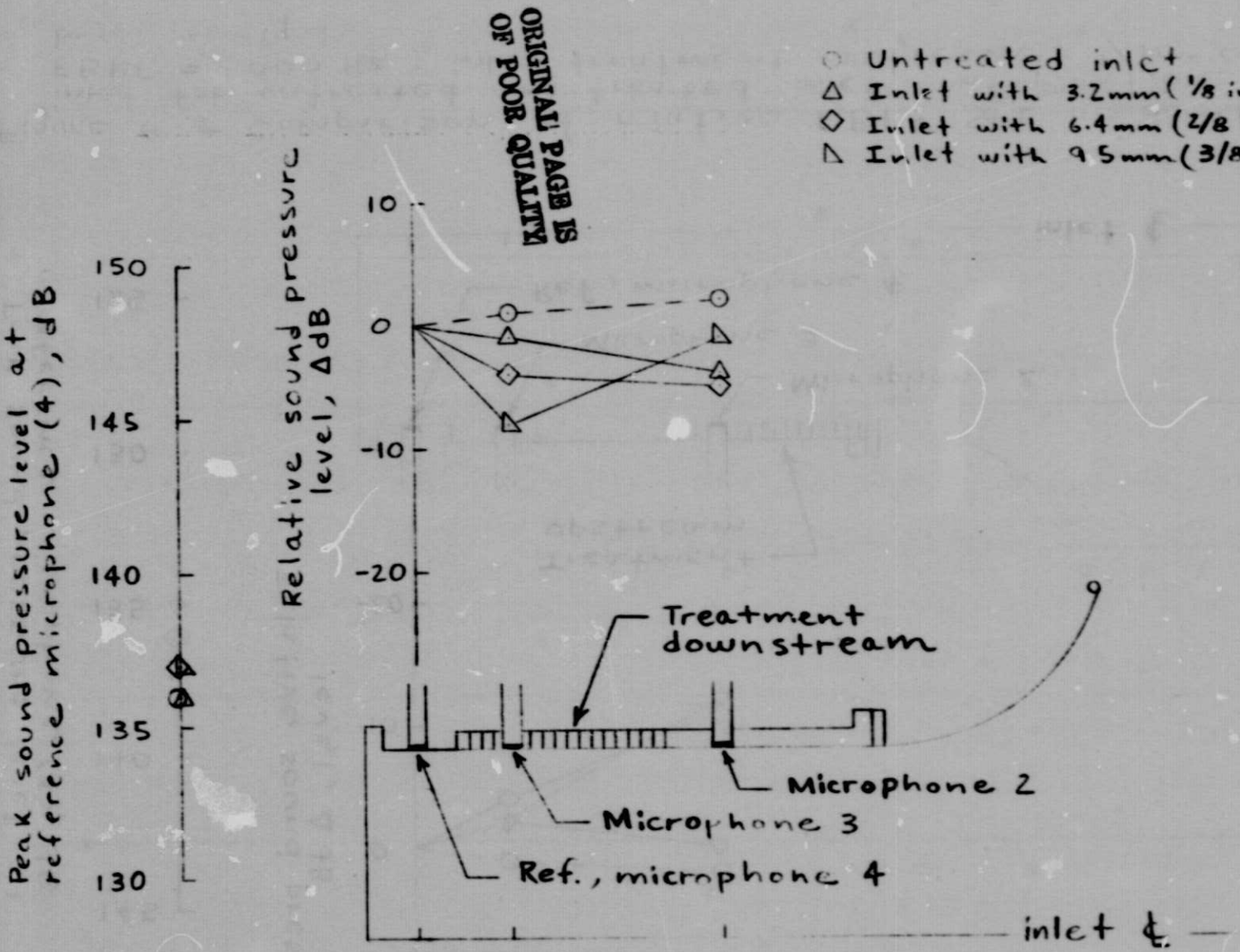

Figure 5.- Comparison of relative FBPF SPL inside compressor inlet for untreated and treated inlet configurations at FBPF = 8000 Hz; inlet treatment downstream; 1/10-octave band analysis.

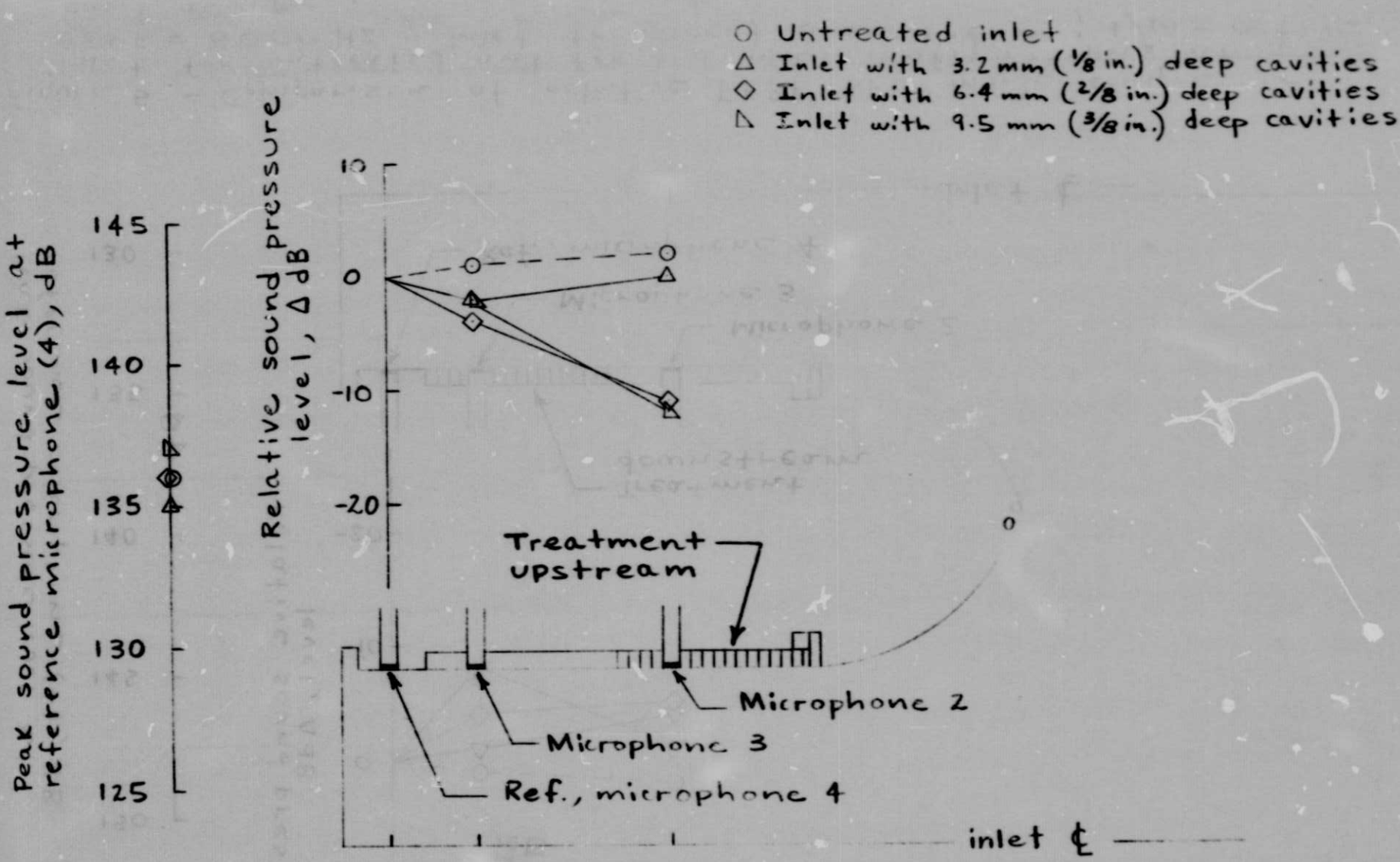

Figure 6. - Comparison of relative FBPF SPL inside compressor inlet for untreated and treated inlet configurations at FBPF = 8000 Hz; inlet treatment upstream; 1/10-octave band analysis.

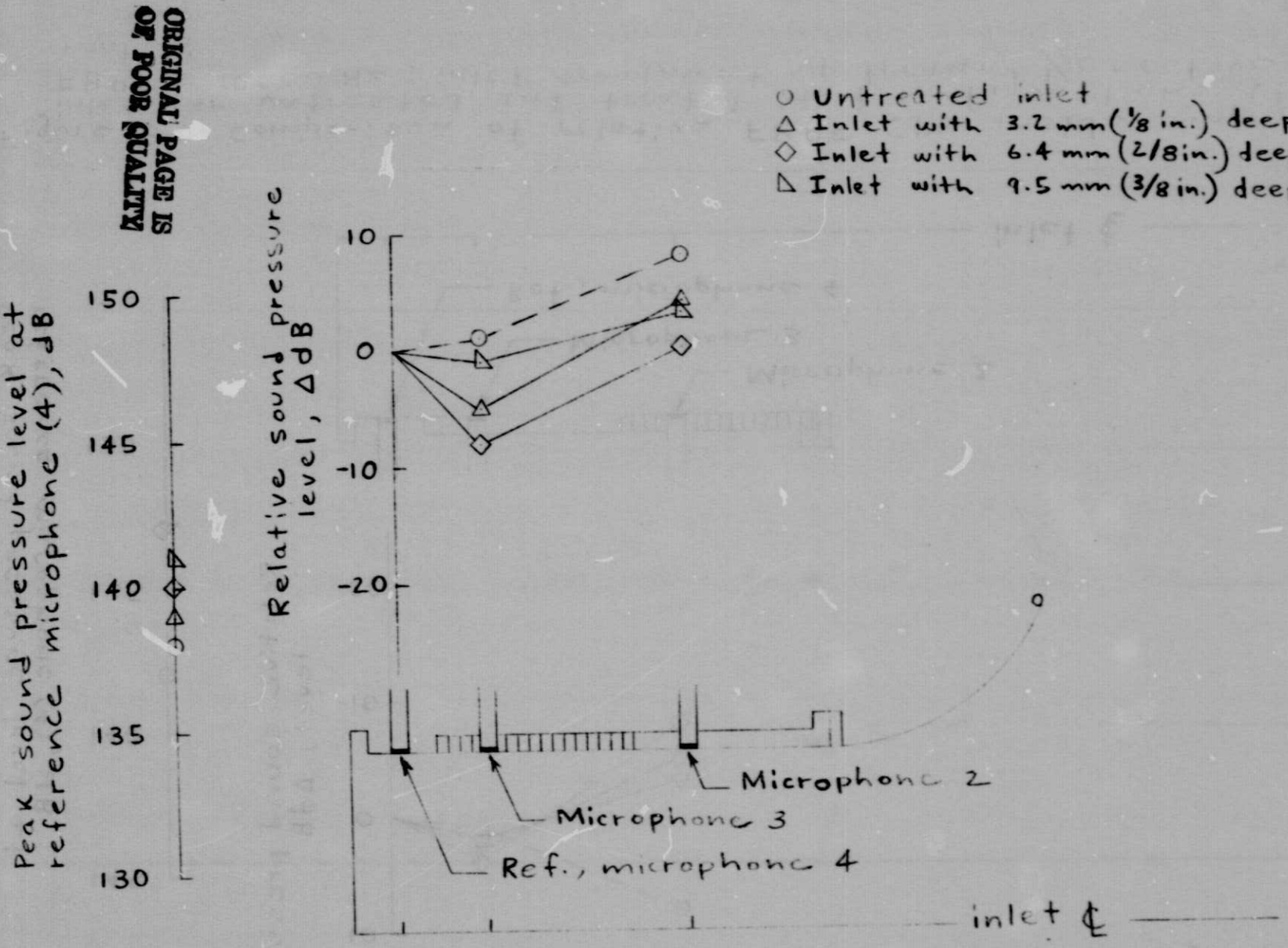

Figure 7.- Comparison of relative FBPF SPL inside compressor inlet for untreated and treated inlet configurations at FBPF = 10000 Hz; inlet treatment downstream; 1/10-octave band analysis.

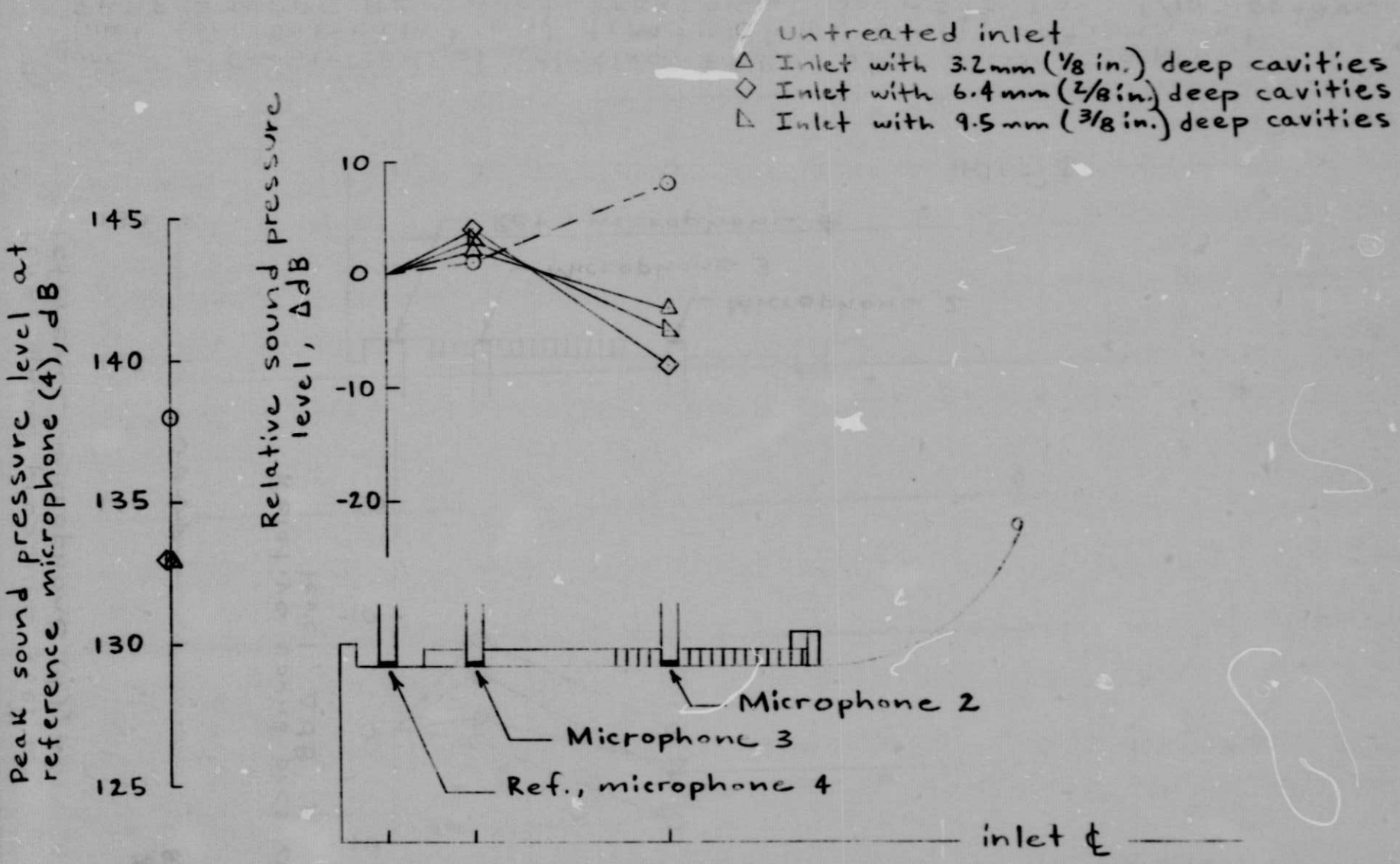

Figure 8. - Comparison of relative FBPF SPL inside compressor inlet for untreated and treated inlet configurations at FBPF = 10000 Hz; inlet treatment upstream; 1/10-octave band analysis.

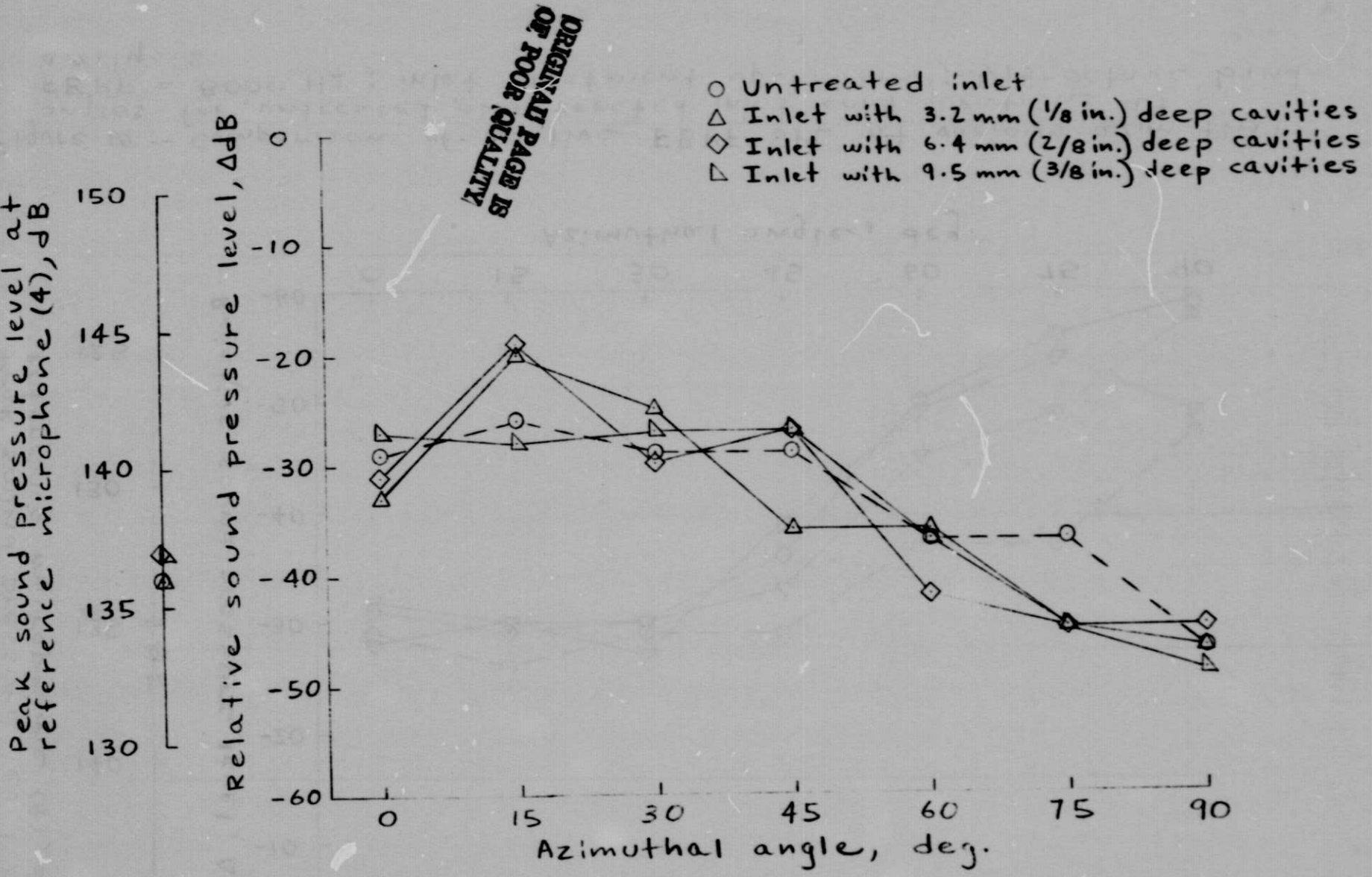

Figure 9. - Comparison of relative FBPF SPL at various azimuthal angles for untreated and treated inlet configurations at FBPF = 8000 Hz; inlet treatment downstream; 1/10-octave band analysis.

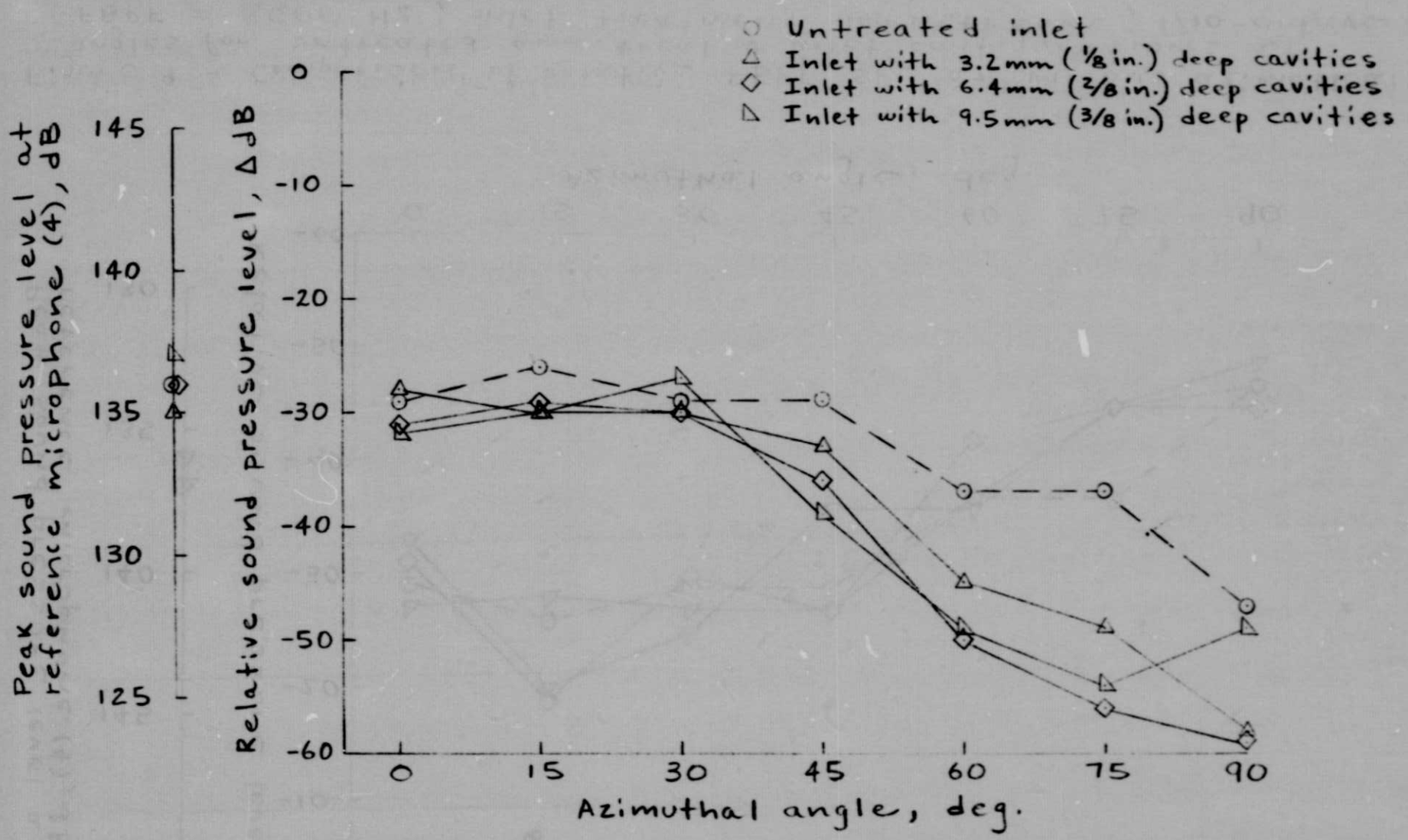

Figure 10.- Comparison of relative FBPF SPL at various azimuthal angles for untreated and treated inlet configurations at FBPF = 8000 Hz; inlet treatment upstream; 1/10-octave band analysis.

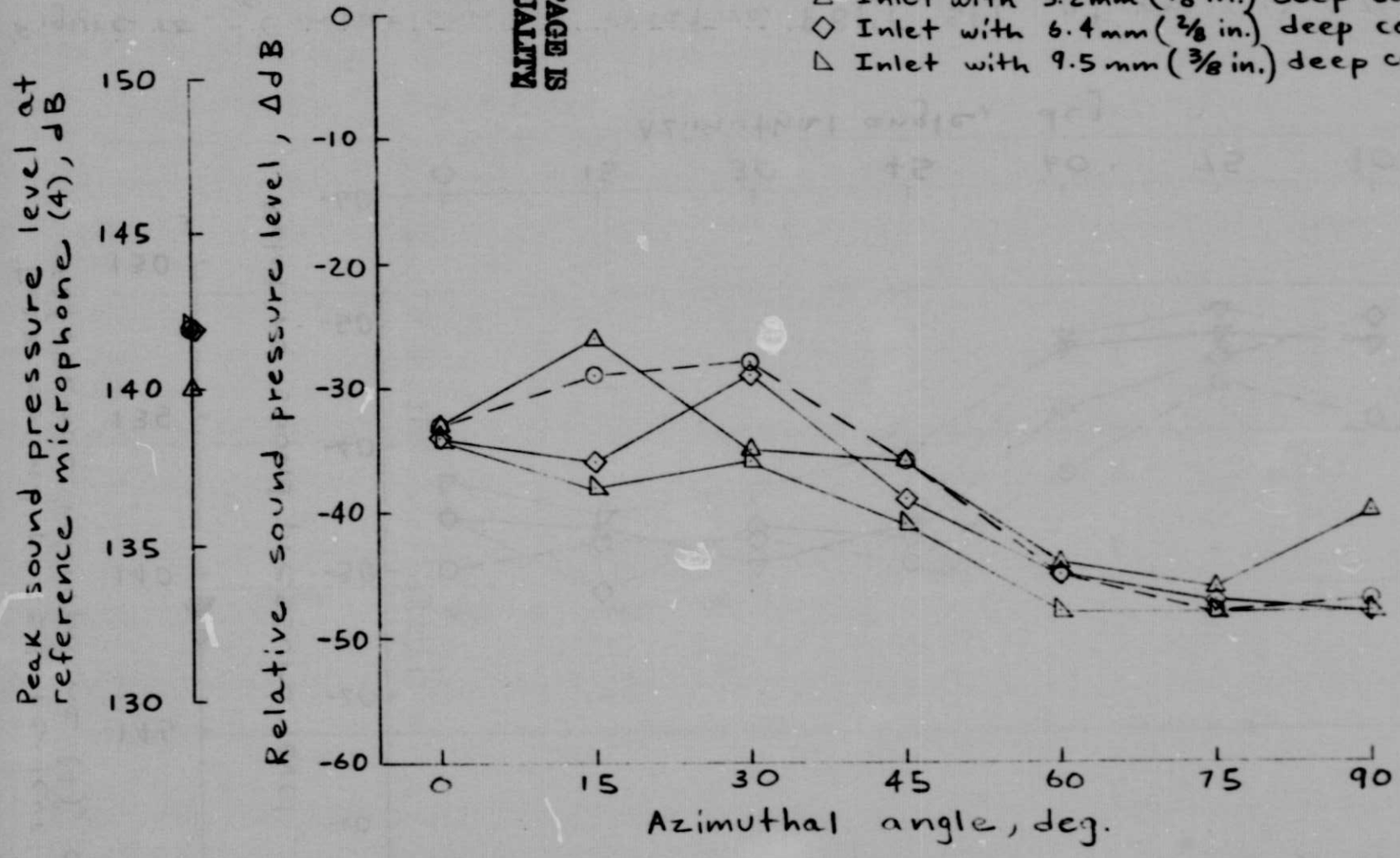

Figure 11. - Comparison of relative FBPF SPL at various azimuthal angles for untreated and treated inlet configuration; at FBPF = 8500 Hz; inlet treatment downstream; 1/10-octave band analysis.

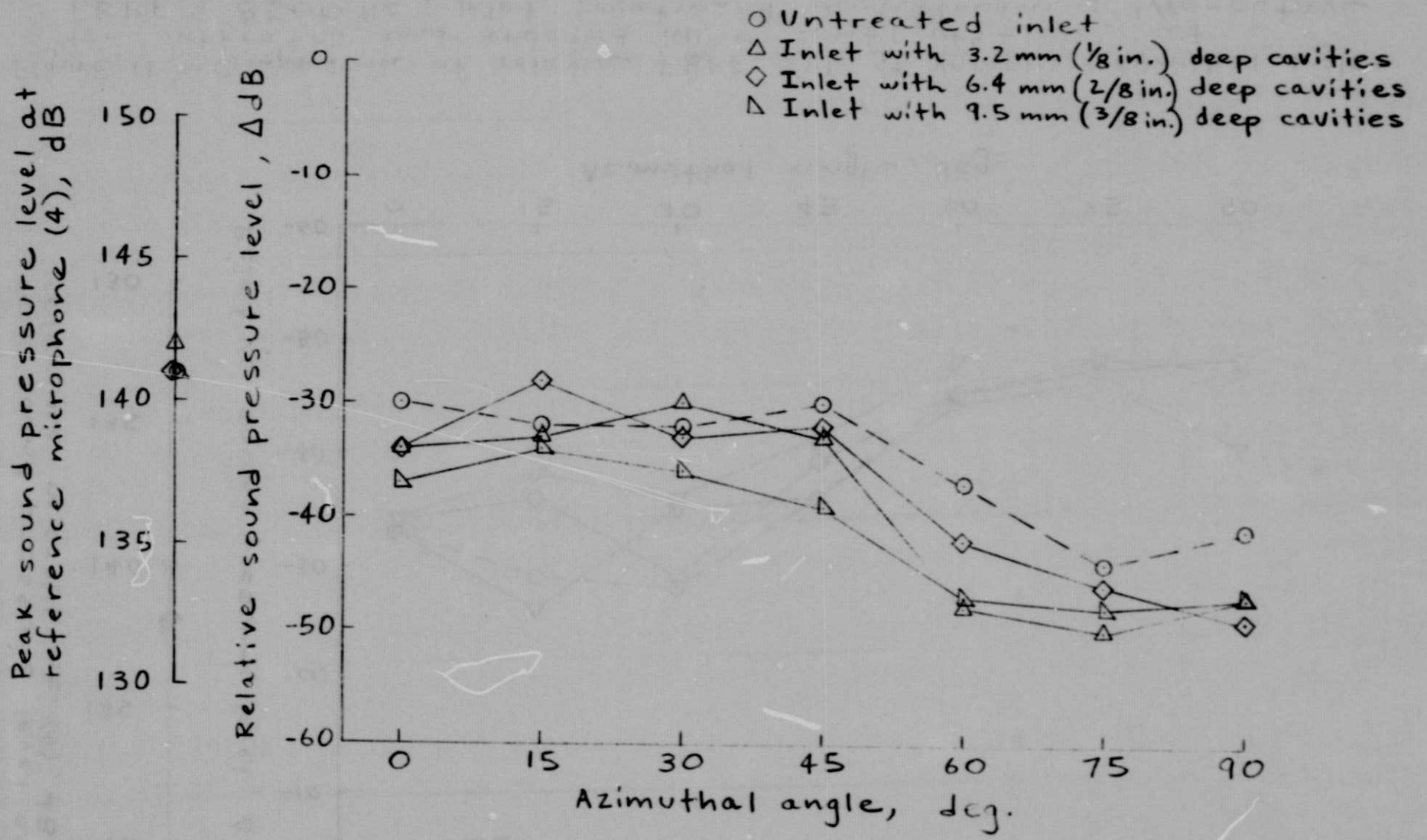

Figure 12. - Comparison of relative FBPF SPL at various azimuthal angles for untreated and treated inlet configurations at FBPF = 9000 Hz; inlet treatment downstream; 1/10-octave band analysis.

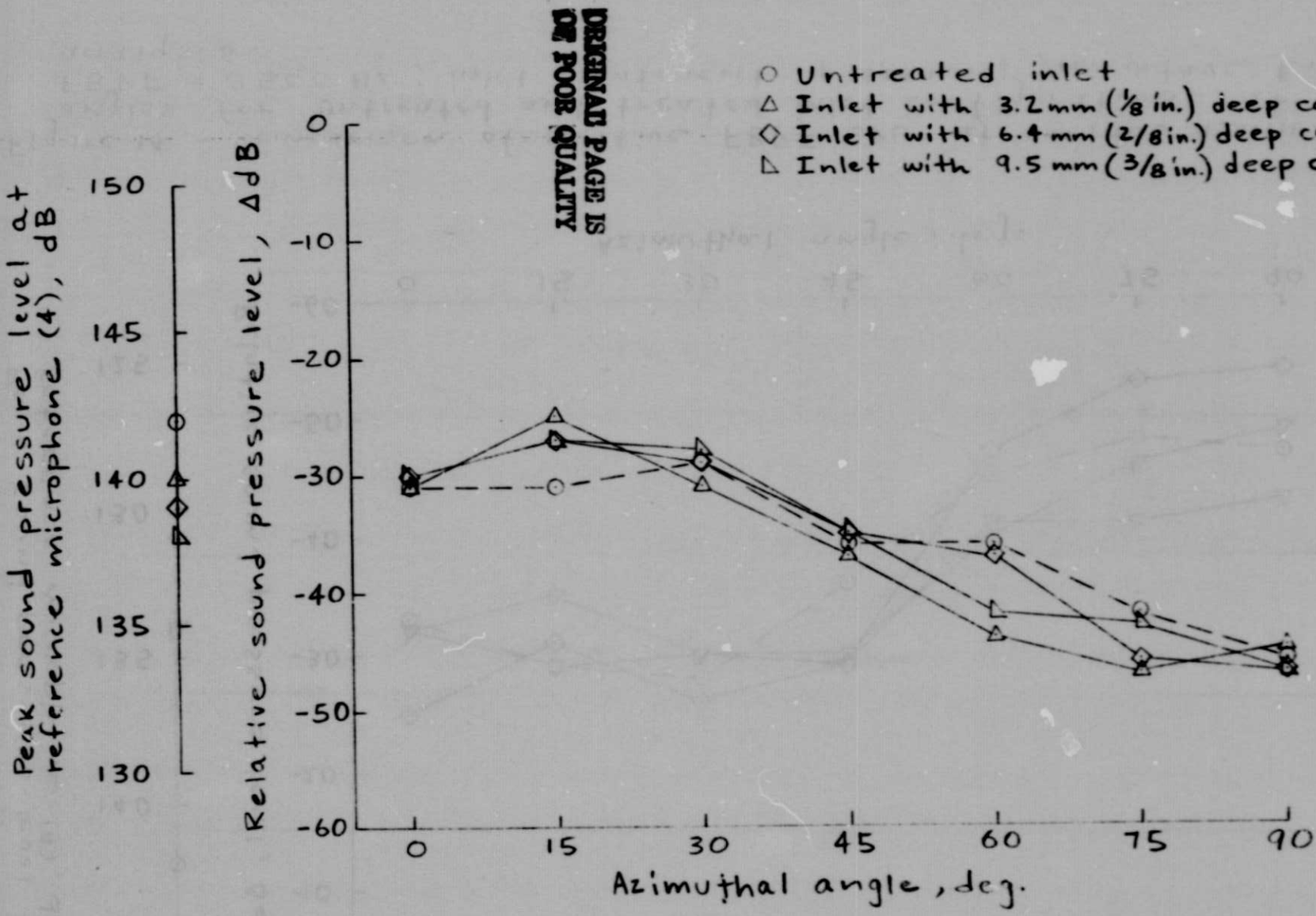

Figure 13.– Comparison of relative FBPF SPL at various azimuthal angles for untreated and treated inlet configurations at FBPF = 9500 Hz; inlet treatment downstream; 1/10 octave band analysis.

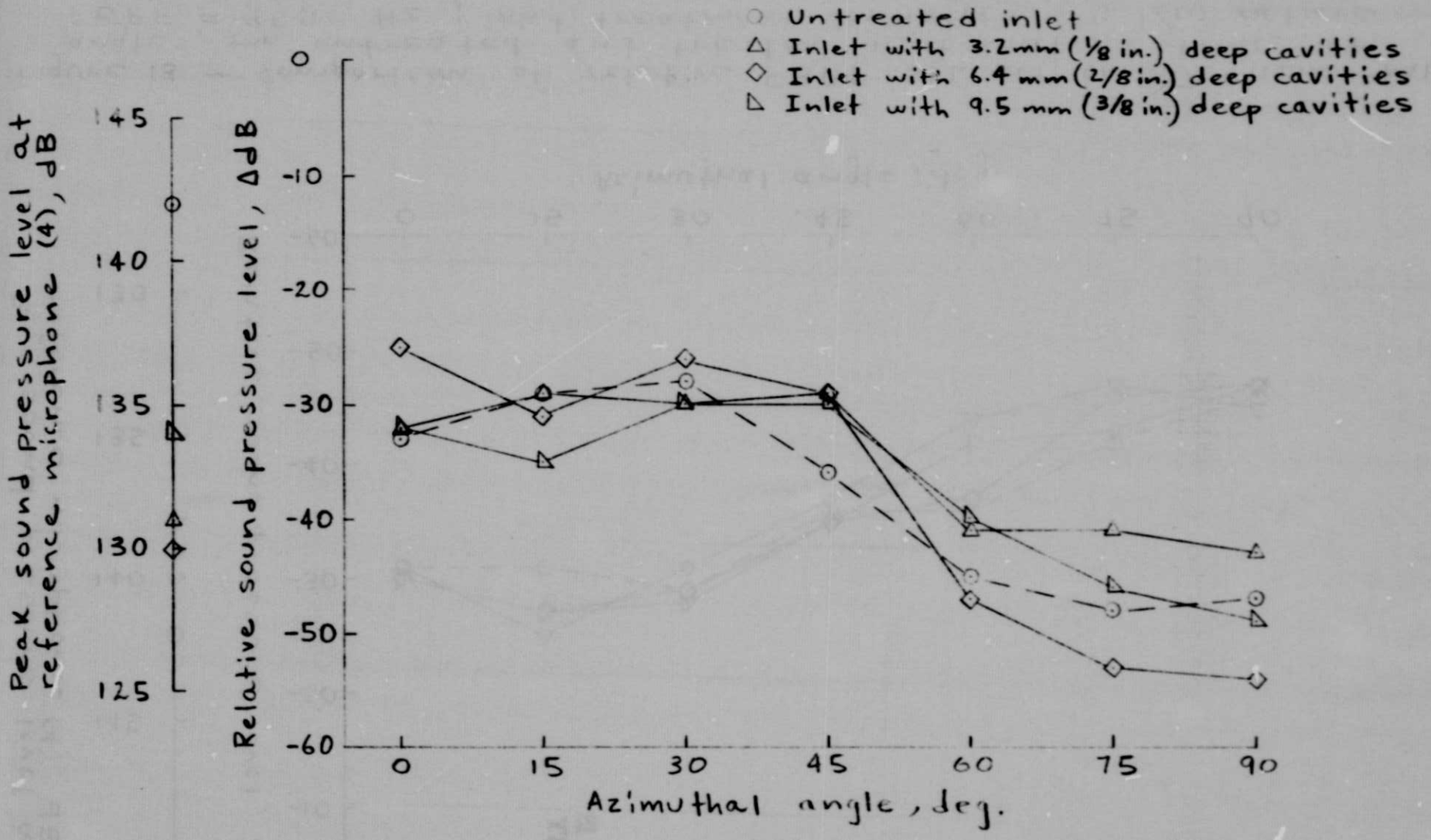

Figure 14.- Comparison of relative FBPF SPL at various azimuthal angles for untreated and treated inlet configurations at FBPF = 8500 Hz; inlet treatment upstream; 1/10-octave band analysis.

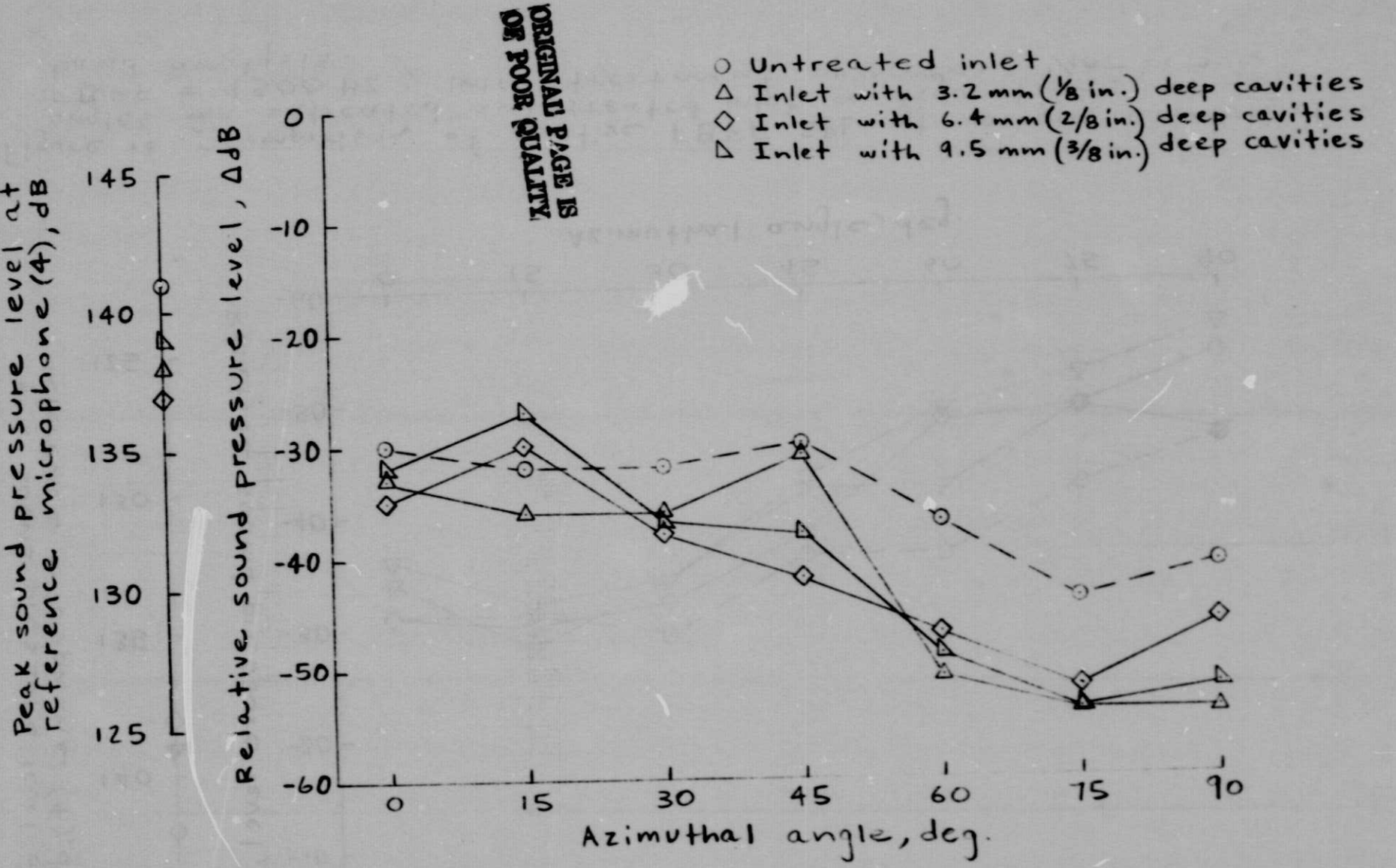

Figure 15. - Comparison of relative FBPF SPL at various azimuthal angles for untreated and treated inlet configurations at FBPF = 9000 Hz; inlet treatment upstream; 1/10-octave band analysis.

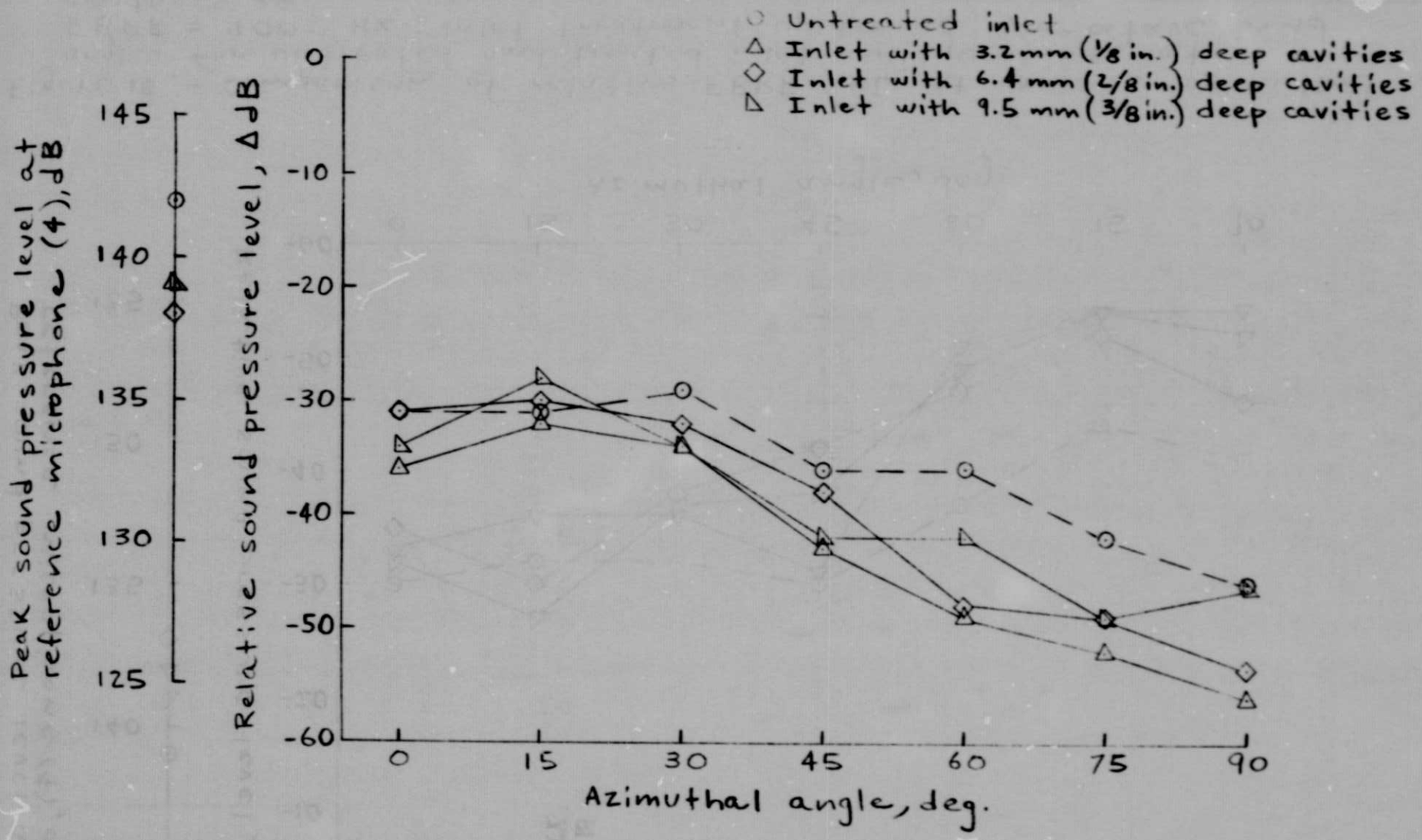

Figure 16. - Comparison of relative FBPF SPL at various azimuthal angles for untreated and treated inlet configurations at FBPF = 9,500 Hz; inlet treatment upstream; 1/10 - octave band analysis.

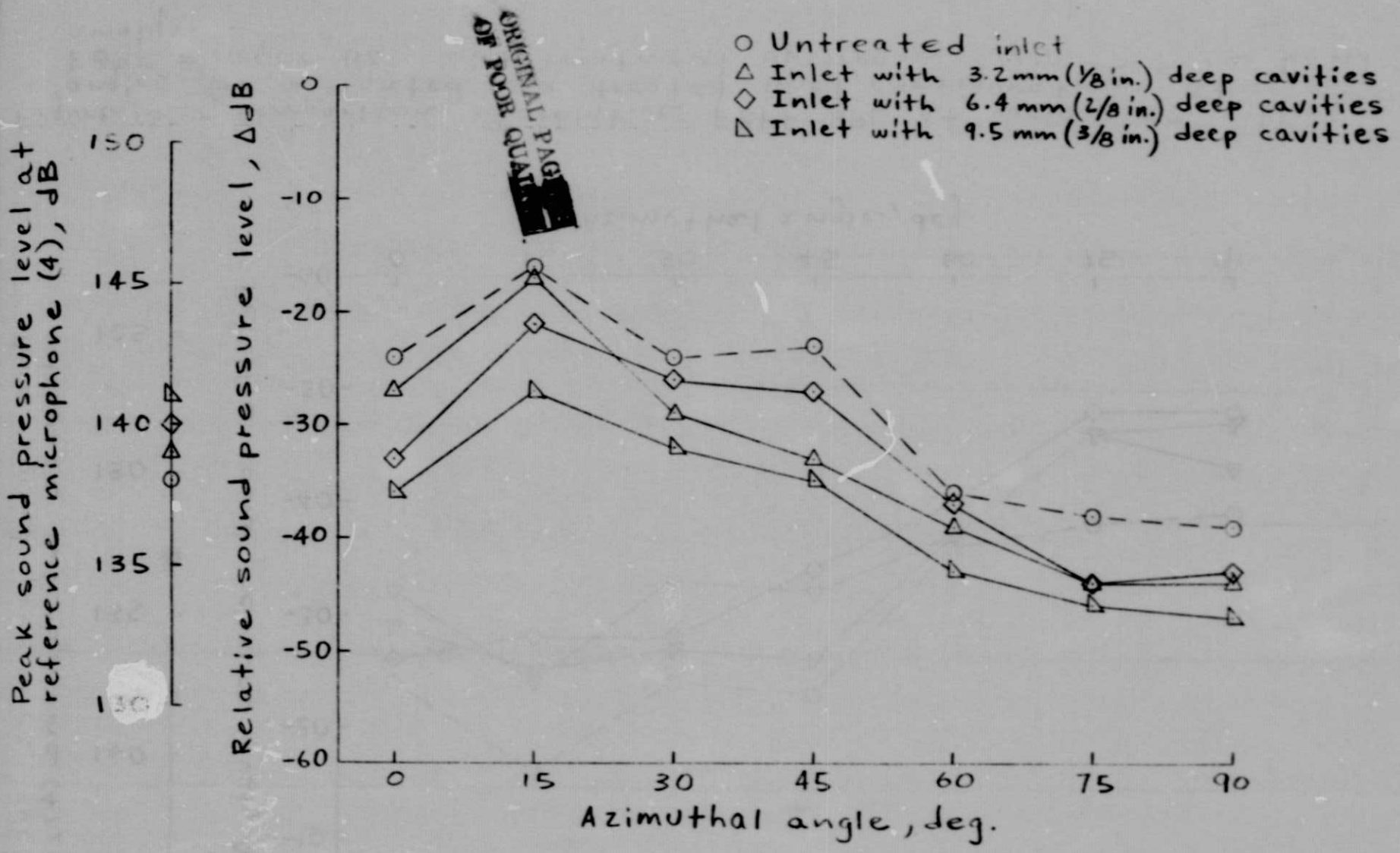

Figure 17. - Comparison of relative FBPF SPL at various azimuthal angles for untreated and treated inlet configurations at FBPF = 10 000 Hz; inlet treatment downstream; 1/10-octave band analysis.

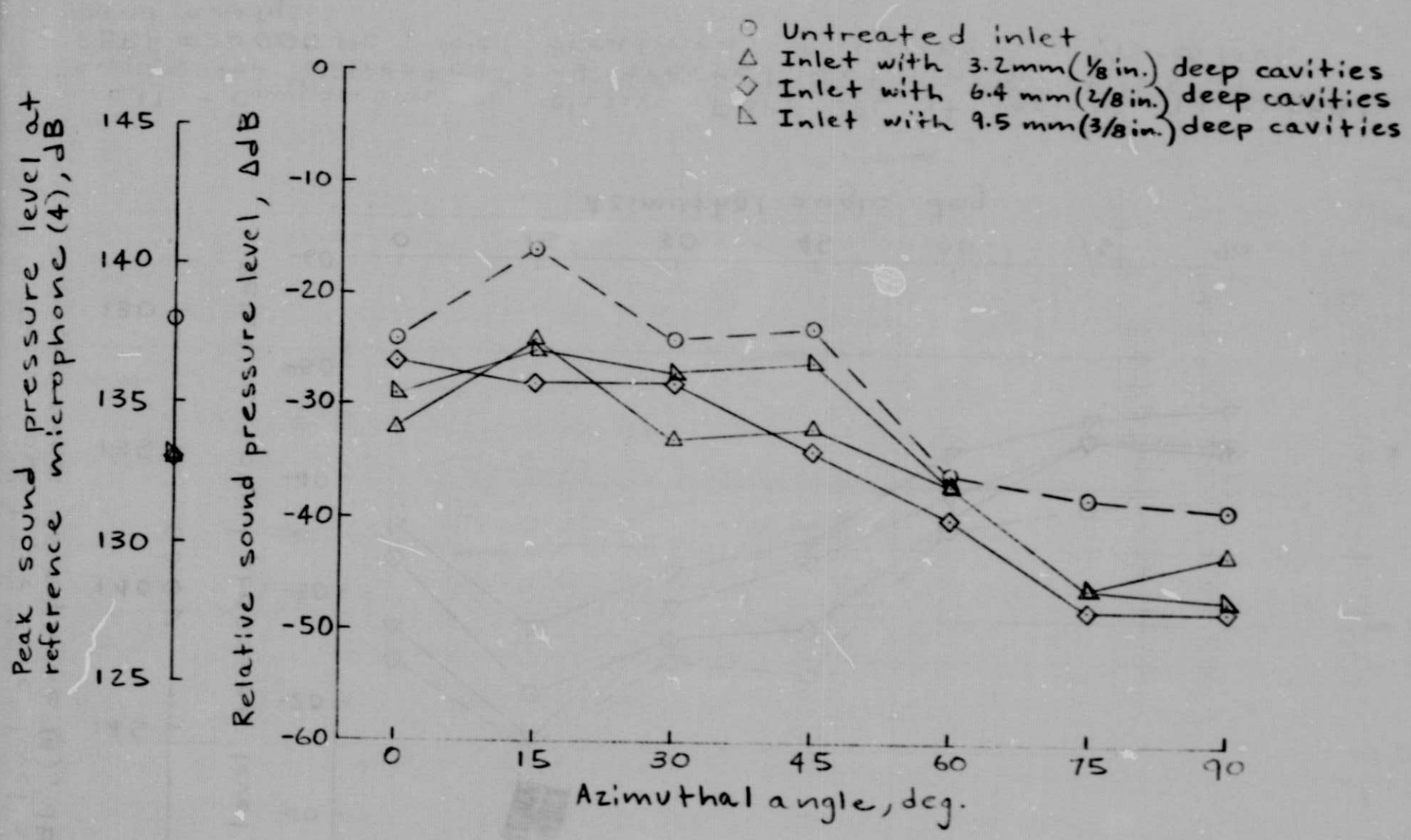

Figure 18. – Comparison of relative FBPF SPL at various azimuthal angles for untreated and treated inlet configurations at FBPF = 10000 Hz; inlet treatment upstream; 1/10 – octave band analysis.

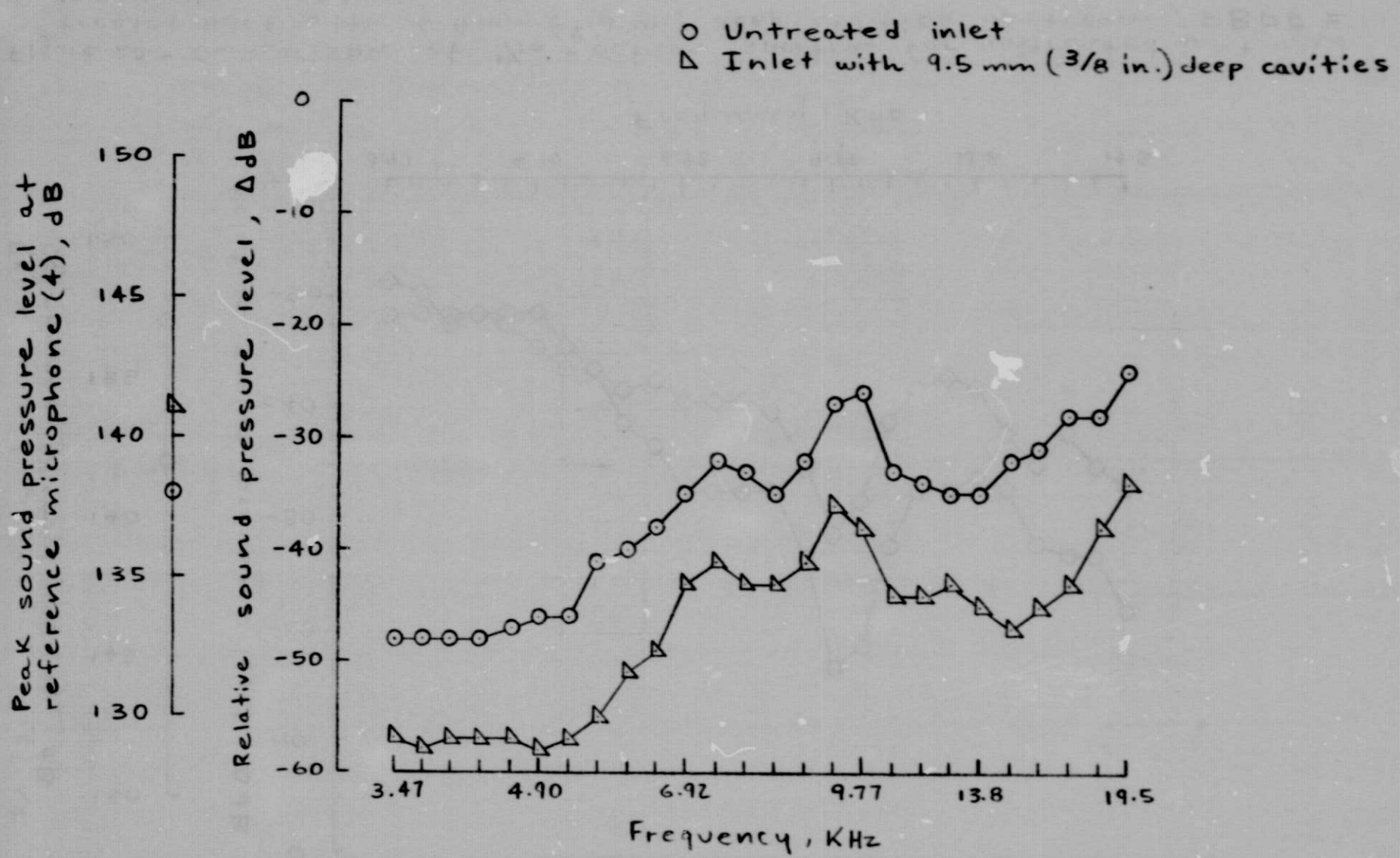

Figure 19.- Comparison of 1/10-octave spectra for untreated inlet and treated inlet with 9.5 mm (3/8 in.) deep cavities downstream; FBPF = 10000 Hz ; 0° azimuth.

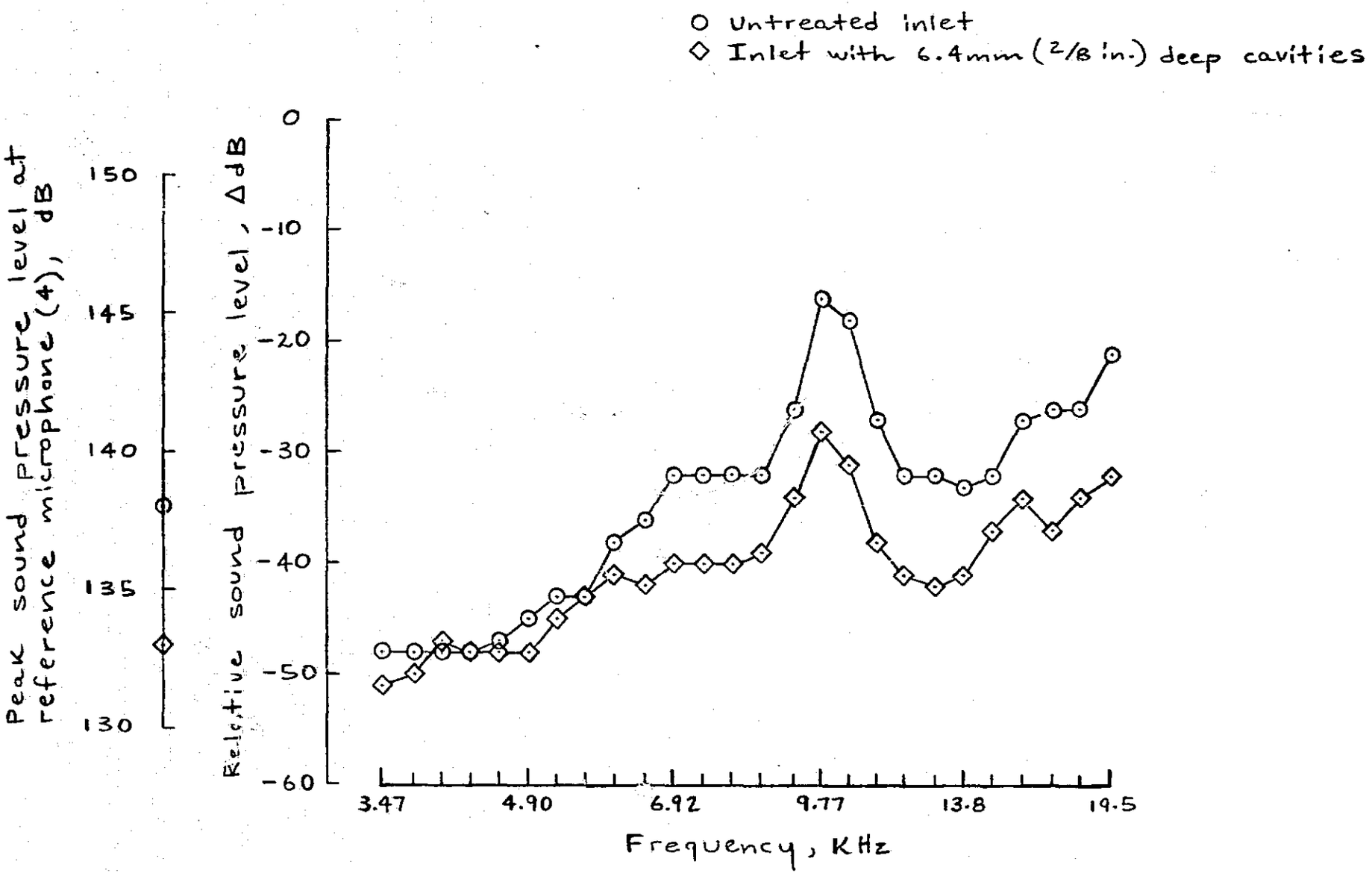

Figure 20.- Comparison of 1/10-octave spectra for untreated inlet and treated inlet with 6.4mm (2/8 in.) deep cavities upstream; FBPF = 10000 Hz; 15° azimuth.

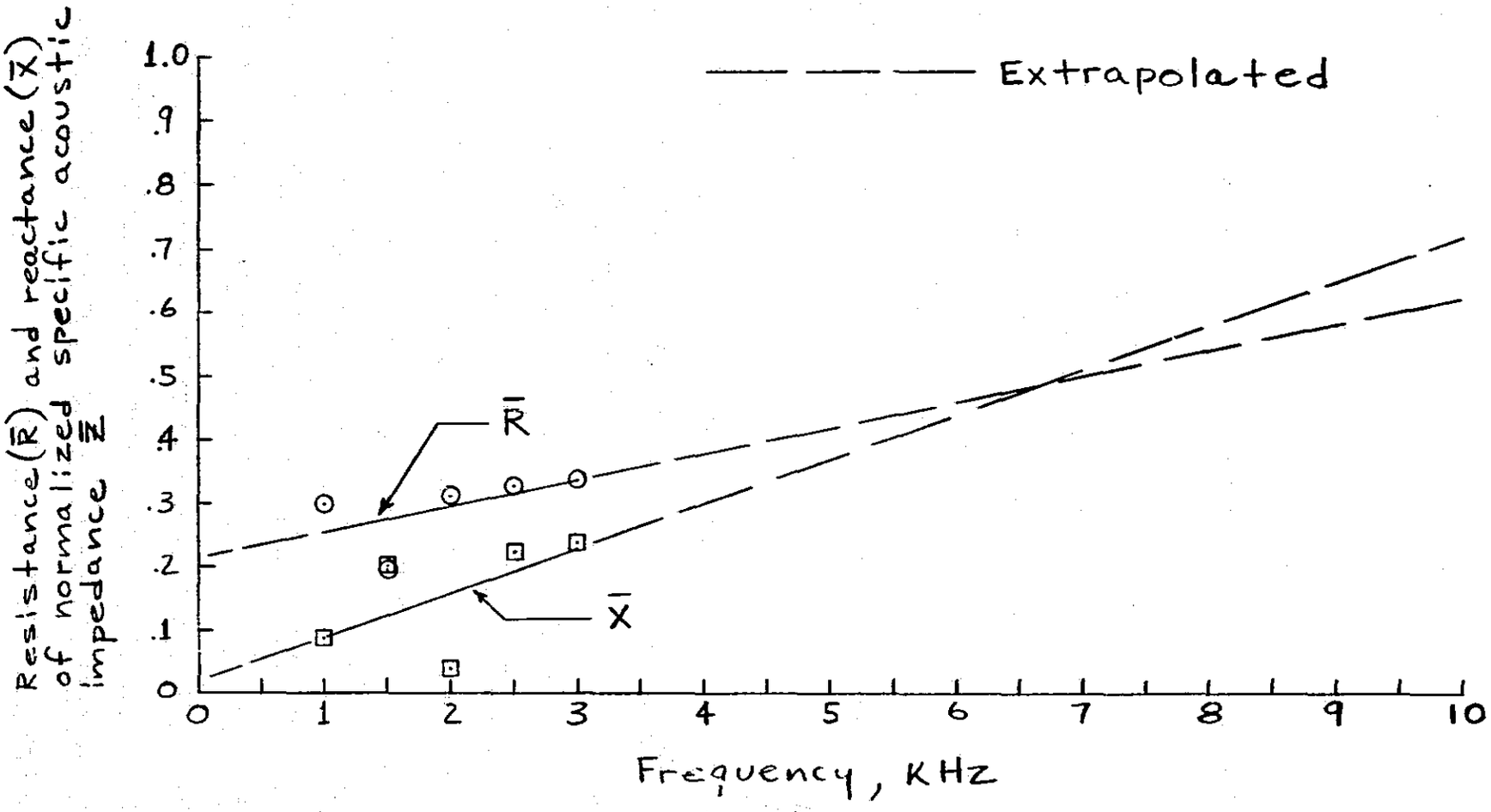

Figure 21.- Normalized specific acoustic impedance of type 347 stainless steel fibermetal at various frequencies.

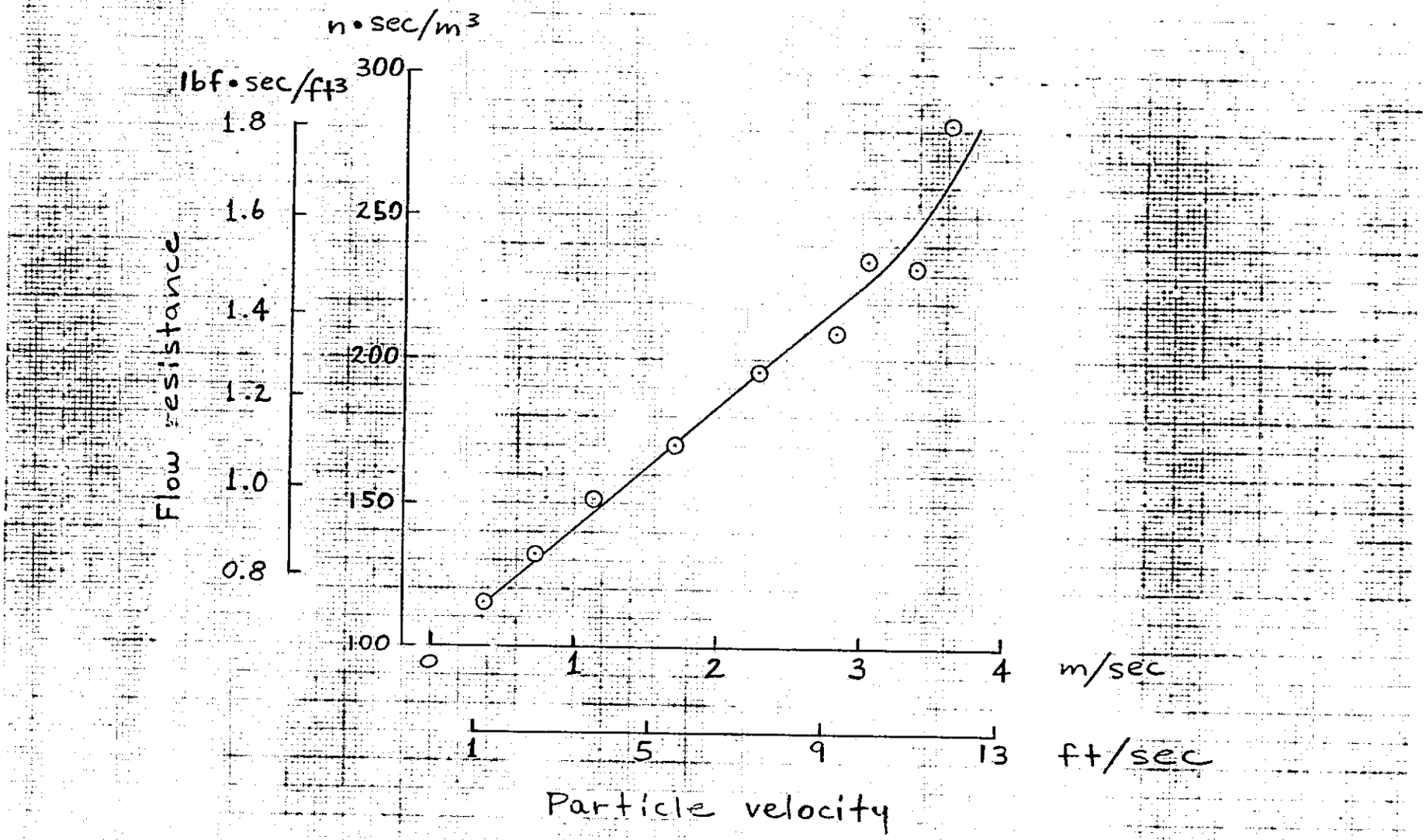

Figure 22. - Flow resistance of type 347 stainless steel fibermetal at various particle velocities.